

Supplemental Material to:

“Universal scaling of the critical temperature for thin films near the superconducting-to-insulating transition”

Introduction to the Supplemental Material:

The following sections give an inclusive list of the values of d , T_c and R_s for some 35 sets of experiments on thin superconducting films in the form of tables and figures. This allows a careful examination of the data, mainly with respect to the scaling presented in the main text.

We present the values of our measurements as well as those collected from published works. These include all the data presented in Fig. 4, along with a few datasets that were not included in Fig. 4.

What is included below?

The datasets for the different superconductors are presented in alphabetic order. Wherever there are multiple sources for a given material, an additional chronological order was used.

Each material is presented with a very brief relevant overview. We then present the raw data for d , T_c and R_s as collected either with DataThief [1] or directly (if applicable) while specifying the actual source (figure/table number in the original report). We also include the data of the films measured and characterized in our lab. For each dataset, we presented the values that we found for A and B by fitting the data to Eq. 1 ($dT_c = A/R_s^B$). We then fed back these values for A and B and also input the thickness and sheet resistance values to extract the corresponding calculated value of T_c for each film, and we present this recalculated value for T_c (T_{c_RC}). Finally, the error of T_{c_RC} with respect to the measured T_c is also presented (‘Err T_{c_RC} %’). The statistical coefficients of determination, R^2 , of the fitting curves to Eq. 1 are also added. In addition to the table of the raw

data, each dataset is displayed graphically in four panels. In the first two panels, T_c is shown as a function of thickness and of the normal state sheet resistance. The third one includes the 3D resistivity, ρ , as a function of thickness. Finally, the scaling of dT_c vs. R_s is presented, while the best fit to Eq. 1 is also drawn when applicable.

As can be qualitatively deduced from Fig. 4, the data agree rather well with the scaling. However, one should bear in mind that the original publications from which the data were extracted did not consider Eq. 1 at all. Thus, despite the good agreement, there are several factors that in some cases made the quantitative analysis somewhat difficult.

Sources of error in the data

(a) Data extraction

In some cases, the data points were taken from several different sources, *e.g.*, from several figures in the original publication, each of which contains only partial data. For instance, the data points were sometimes reconstructed from two independent figures in the original publication, one graph of $T_c(d)$ and one of $T_c(R_s)$. Hence, errors have already accumulated in the data extraction process. We evaluated this error in the following way. After extracting the values for d , T_c and R_s from the two sources, the error in the values that were extracted more than once were calculated. Bearing in mind the example of data extracted from two independent graphs of $T_c(d)$ and of $T_c(R_s)$, the difference in the values of T_c can be calculated to evaluate the error in the data extraction process. We presented these values below, designated by “Err $d\%$ ”, “Err $T_c\%$ ” and “Err $R_s\%$ ”. In these cases, if the cross-checked values resulted in a low level of confidence for some data points, these data points were presented (and highlighted) but were not taken into consideration for the quantitative analysis.

(b) Thickness measurements

Another error source is the low certainty accompanied with the determination of the measured values of ultrathin films. In particular, in most cases, the thickness is measured indirectly. Typically, this is done by measuring the frequency shift on a quartz oscillator that is located close to the substrate and then calculating the volume, and hence the thickness of the deposited material, given that the density of the material and the relevant geometrical factors are known.

(c) Films thinner than a single unit cell

In some cases, the reported thickness of the films was smaller than a single unit cell of that material. Hence, for these sets of films, we considered only films that are thicker than one unit cell size.

(d) Inhomogeneity of films within a given set

In addition, for the analysis we did, we assumed that films that belong to the same dataset are similar in nature. Nevertheless, in many cases, films within the same dataset vary according to different parameters that are not always reported or able to be detected, such as stoichiometry, strain, grain size, dopant concentration, physical dimensions, etc. Therefore, such unknown variations between films within the same dataset are likely to encumber the quantitative analysis of the data. In fact, in some cases, it was specified explicitly that the growth conditions were changed from one film to another for different reasons (*e.g.*, for optimizing T_c)

(e) Homogeneity within a given film

Another potential source of error in the values reported for the measured values (mainly for the thickness) is the homogeneity of the material within a given film. In some cases, it is impractical to examine the homogeneity of the superconductor with respect to, *e.g.*, the granularity of the

material, the distribution of chemical or magnetic contaminations, and the homogeneity of the thickness (*e.g.*, films reported to be thinner than a unit cell cannot have constant thickness across the samples). Hence, this might lead to inconsistency in the results.

(f) Reported in low level of confidence

In several cases, the authors who report the values of the film they measured add a note regarding to certain films (usually the thinnest films), in which they suggest that the values measured for these films should be considered in cautious. For instance, this can be due to one or more of the reasons specified above. In such cases, we specified these values below. However, we did not consider these films for the quantitative analysis.

(g) Incomplete or irrelevant data

Since we wanted to examine the relations between R_s , T_c and d , we looked only at the data sets in which all these three values were measurements for enough films from that set. We give some examples below for paper that we omitted from the current survey, as some of the reported values were nominal, rather than measured. For instance, several studies that explored superconductivity in Bi films reported the values measured for T_c and R_s , while the values reported for d , were nominal based on the assumption that the resistivity is constant for all of the films. Hence, we did not consider these papers.

Likewise, some work on thin film superconductivity deals with ‘unconventional’ superconductors. For instance, this can include a layered material, which is composed of two different materials. Examples for this are the work by Strunk *et al.* on layered Nb/Gd films [2], and the work by Kapitulnik and co-authors on layered MgB₂/MgO films [3].

The fact that most of the datasets agree both quantitatively and qualitatively with the universal scaling despite these hurdles strengthens the fact that the reported power law is universal. The above factors can usually allow a sufficient explanation wherever there is a deviation from the scaling of Eq. 1. Below, we analyzed each of the datasets and specified the factors that may have affected the quantitative analysis, wherever applicable.

1. Aluminum.

The scaling of superconductivity in thin Al films is unique in the sense that T_c is enhanced rather than suppressed. That is, unlike in most other superconductors, the reported T_c in thin aluminum films usually exceeds its bulk value (T_c of the bulk: ~ 1.2 K [4]). Moreover, the value of T_c in Al generally increases with decreasing thickness. Hence, the fact that the scaling of Eq. 1 fits the data for Al is presumably a surprise. We present here data collected on superconductivity in aluminum by three independent studies, and it should be noted that the third dataset is one of the only cases where Eq. 1 does not fit the data very well.

It is interesting to point out that the exponents for the two cases where Eq. 1 fits the data are of the smallest values among the examined materials ($B < 0.5$).

1.1. Aluminum (Cohen and Abeles [5], \diamond in Fig. 4).

An early report (1968) by Cohen and Abeles [5] demonstrated a continuous enhancement of T_c with decreasing thickness in aluminum. This increase resulted in T_c higher than that of the bulk value (T_c of the bulk: ~ 1.2 K [4]).

Table S1.1. Superconductivity in aluminum films (Cohen and Abeles [5]), \diamond in Fig. 4. d , T_c , and R_s (the latter was measured at 4.2 K) reproduced from Table 1 of Cohen and Abeles [5], as well as the values calculated for A , B , T_{c_RC} , and Error in T_{c_RC} %.

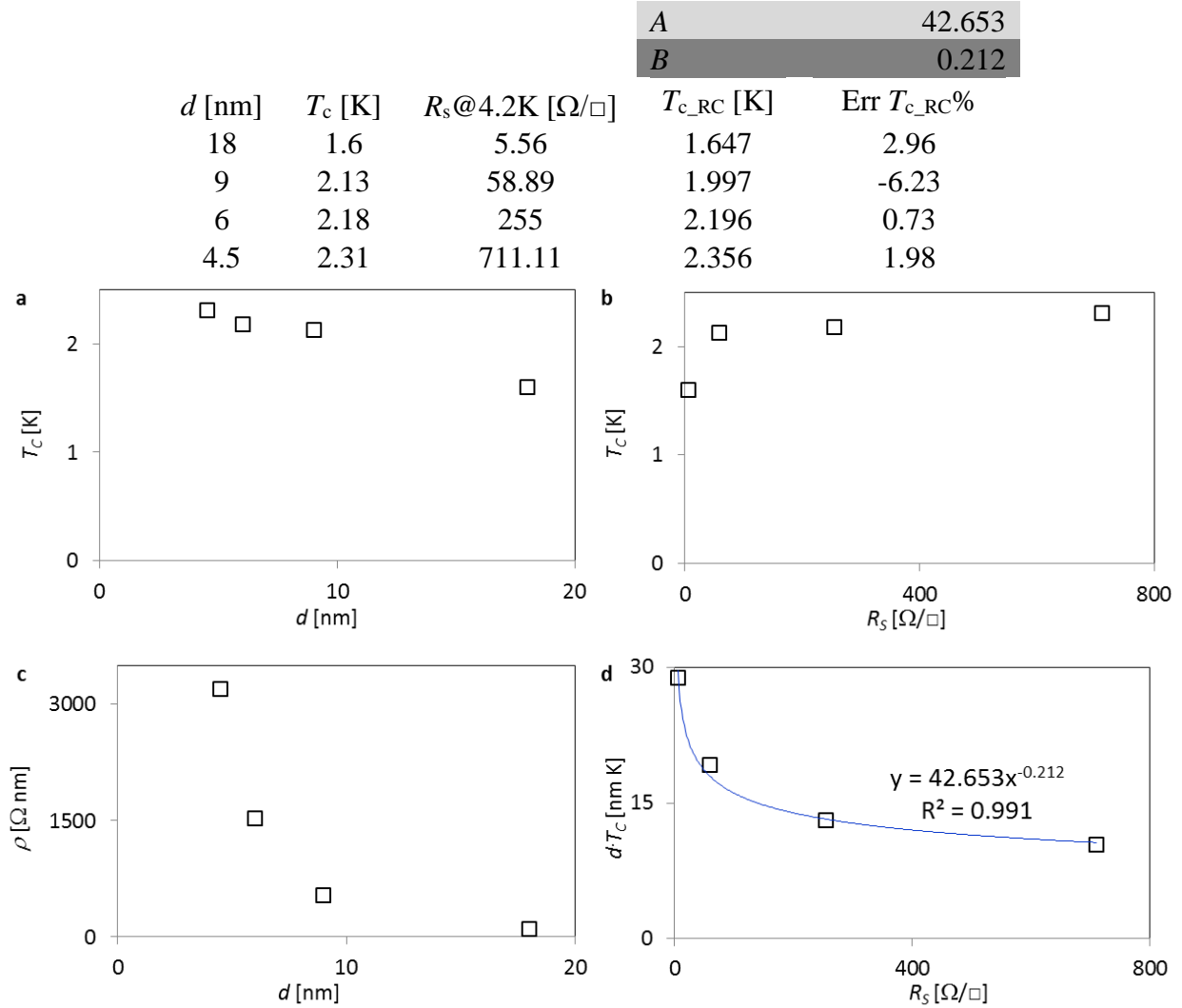



Figure S1.1. Superconductivity in aluminum films (Cohen and Abeles [5]), \diamond in Fig. 4. Critical temperature as a function of (a) thickness and (b) sheet resistance indicates enhancement of T_c with decreasing thickness. (c) Resistivity as a function of thickness. (d) dT_c vs. R_s fits to Eq. 1 with $A = 42.653$, and $B = 0.212$.

1.2. Aluminum (Strongin *et al.*, [6] in Fig. 4).

Following Cohen and Abeles' experiments, Strongin *et al.* observed a similar increase in T_c for thinner film, but here T_c started to drop down below $d = 2.4$ nm (which corresponds to $R_s = 803\Omega/\square$). Yet, in all films, the measured T_c was higher than the bulk value. Despite this dissimilarity, this dataset also agrees with Eq. 1.

Table S1.2. Superconductivity in aluminum films (Strongin *et al.* [6]),  in Fig. 4. d , T_c , and R_s from the two panels of Fig. 1 from Strongin *et al.* [6] as well as the values calculated for A, B, T_{c_RC} , and Error in $T_{c_RC}\%$. Since the data points were matched through a common thickness value, the difference in d extracted from the two panels is also added ('Error in $d\%$ ')

Taken from Fig. 1 Top	Taken from Fig. 1 Top	Taken from Fig. 1 Bottom	Taken from Fig. 1 Bottom		A	192.43
d [nm]	T_c [K]	d [nm]	R_s [Ω/\square]	Err $d\%$	B	0.431
					T_{c_RC} [K]	Err $T_{c_RC}\%$
1.503	2.989	1.527	5996	1.59	3.01	1.38
2.389	4.591	2.412	803	0.98	4.51	-3.42
3.299	4.496	3.321	364	0.69	4.59	2.84
4.202	4.416	4.233	226	0.73	4.43	0.31
6.324	4.110	6.313	100	-0.18	4.18	1.1
8.400	3.716	8.4	70.114	-0.01	3.67	-0.56

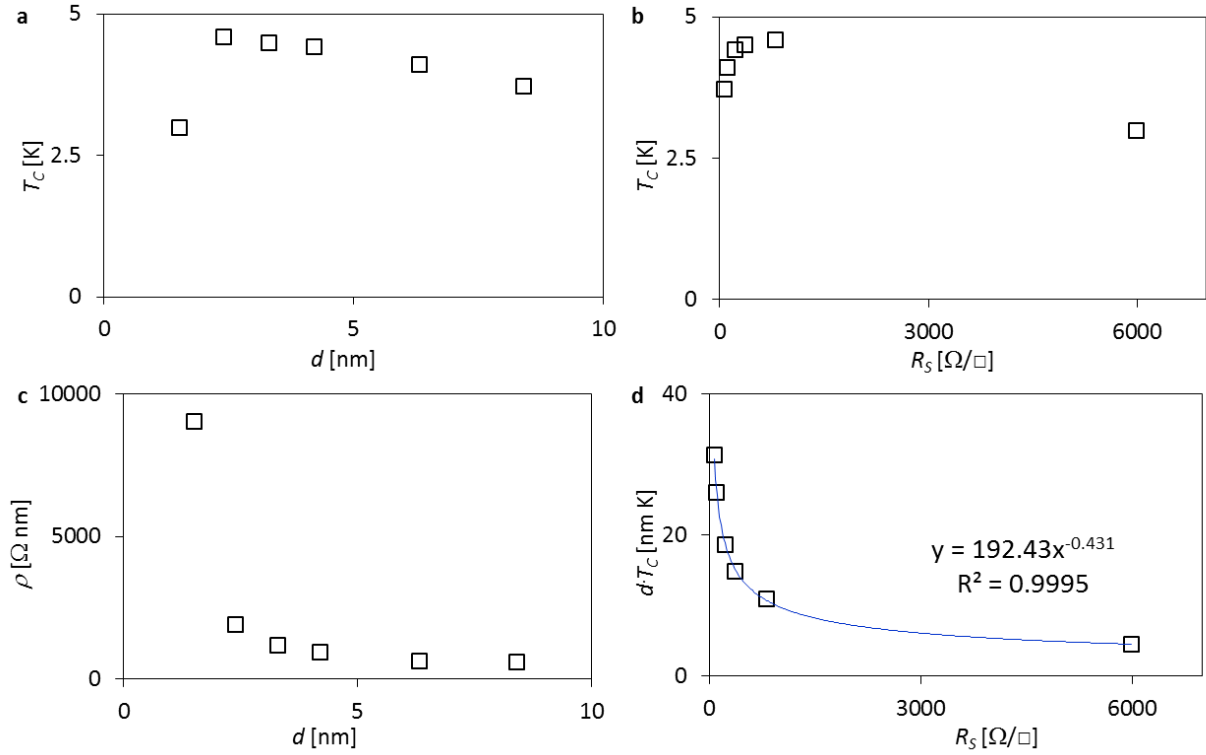


Figure S1.2. Superconductivity in aluminum films (Strongin *et al.* [6]), \blacklozenge in Fig. 4. Critical temperature as a function of (a) thickness and (b) sheet resistance indicates enhancement of T_c with decreasing thickness, while the trend changes at $d = 2.4$ nm ($R_s = 803 \Omega/\square$). (c) Resistivity as a function of thickness. (d) dT_c vs. R_s fits to Eq. 1 (blue curve) with $A = 192.43$, and $B = 0.431$.

1.3. Aluminum (Liu *et al.* [7])

A later paper by Goldman and co-authors repeated the previous measurements but with samples grown in somewhat cleaner conditions. Similarly to the case of Strongin *et al.*, although T_c assumed values larger than the bulk, it started decreasing at a certain thickness ($d = \sim 4.2$ nm), while here it even went below the bulk T_c (at $d < \sim 2.5$ nm). On the other hand, the dependence of T_c on R_s was found to be rather linear. When plotting dT_c as a function of R_s , one obtains a smooth monotonic function as in the other superconductors. However, this function decreases much more

slowly than a power law (the decrease is approximately logarithmic) and does not agree with Eq. 1. A possible partial reason for this is the large uncertainty in the values of d , R_s and T_c . Another possible deviation of this dataset from the framework of Eq. 1 might be related to the thickness measurement or more likely, to the Ge substrate used for these films as was discussed by the authors. Specifically, the proximity effect could have played a significant role in changing the superconducting properties of the Al films grown on the Ge substrate. Although the scaling of Eq. 1 was found to agree well with the data of Bi and Pb films grown in the same method (Fig. S2.1 and S12.7), the proximization may have influenced the Al films over a larger thickness scale. A more insightful discussion about these thin aluminum films is given in Section 17.2.

Table S1.3. Superconductivity in aluminum films (Liu *et al.* [7]). d , T_c , and R_s from the two panels of Fig. 9 from Liu *et al.* [7] Since the data points were matched through a common T_c value, the difference in T_c extracted from the two panels is also added (‘Error in measured $T_{c_RC}\%$ ’), which was found to be relatively large.

Taken from Fig. 9 Top T_c [K]	Taken from Fig. 9 Top $1/d$ [$1/\text{\AA}$]	Taken from Fig. 9 bottom T_c [K]	Taken from Fig. 9 bottom $R_s@14K$ [Ω/\square]
0.544	0.0415	0.535	16889.76
0.942	0.0402	0.936	15291.92
1.209	0.0398	1.202	13989.39
1.408	0.0393	1.4	12881.26
1.434	0.0374	1.471	12478.31
1.476	0.039	1.425	11083.42
1.495	0.0371	1.486	10486.34
1.936	0.0369	1.932	9808.783
2.068	0.0368	2.064	9182.692
2.151	0.0352	2.167	8901.873
2.167	0.0357	2.163	8686.155
2.270	0.0348	2.144	8549.596
2.360	0.0342	2.259	8254.349
2.408	0.0335	2.355	7815.351

2.534	0.0333	2.407	7398.089
2.617	0.0322	2.525	6930.246
2.669	0.0313	2.615	6591.946
2.788	0.0308	2.66	6260.998
2.858	0.0287	2.785	5836.278
2.878	0.0297	2.875	5426.068
3	0.0285	2.859	5059.385
3.121	0.0282	2.997	4699.338
3.147	0.0275	3.122	4396.865
3.26	0.027	3.147	4130.706
3.337	0.026	3.263	3813.886
3.439	0.0165	3.34	3525.969
3.442	0.02	3.333	3159.251
3.459	0.0248	3.452	2899.948
3.481	0.0242	3.478	2669.743
3.507	0.0226	3.535	2439.424
3.516	0.0165	3.535	1605.269
3.533	0.0211	3.451	1346.694
3.545	0.0193	3.55	1159.369
3.546	0.0236		
3.578	0.022		

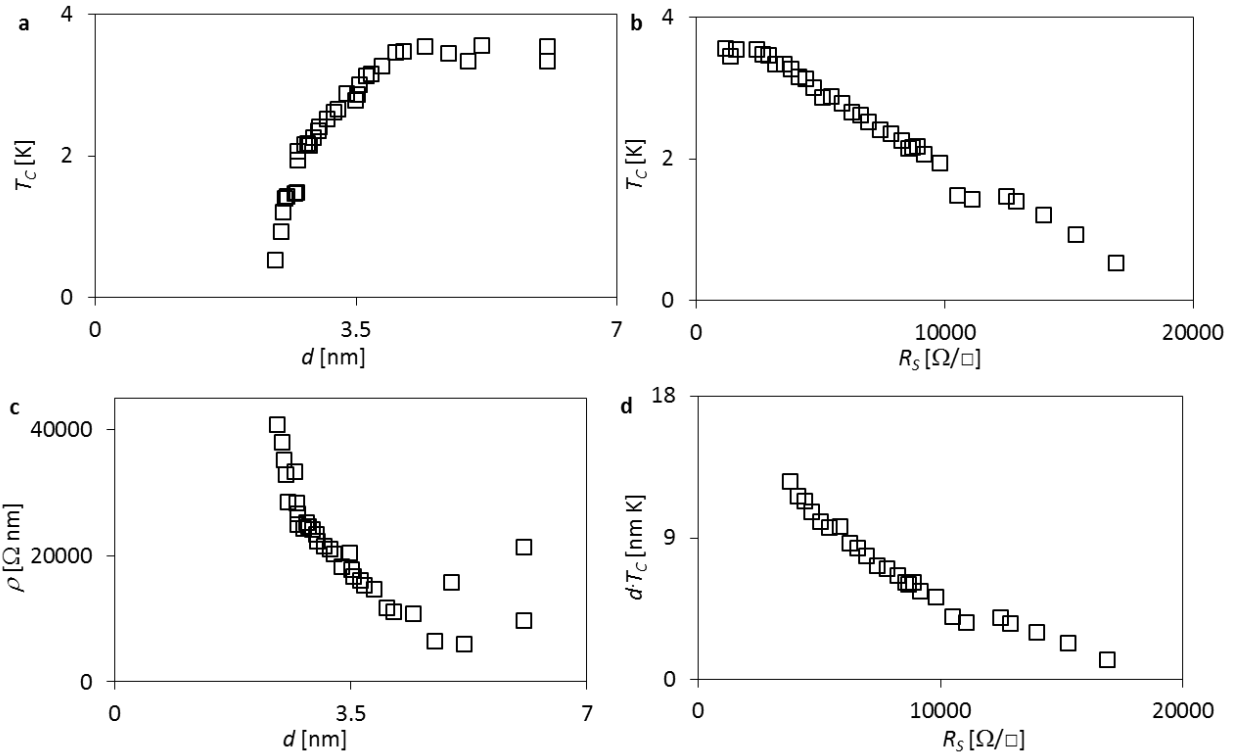


Figure S1.3. Superconductivity in aluminum films (Liu *et al.* [7]). (a) Critical temperature as a function of thickness indicates a slow decrease of T_c with decreasing thickness, while the value of T_c falls to the bulk value at $d = \sim 2.5$ nm. (b) T_c vs. sheet resistance demonstrates a rather linear dependence. (c) Resistivity as a function of thickness. (d) dT_c vs. R_s decreases monotonically but much more slowly than the power law of Eq. 1.

2. Bismuth.

A classic example for superconducting-insulator quantum transition, Bi is an interesting material for testing the scaling of Eq. 1. Unfortunately, most published data on Bi are either incomplete or irrelevant. For instance, Landau *et al.* tried to proximitize Bi in a special way [8], while Silverman only assumed the values for the thickness without actually measuring it in two papers [9,10] and the data published by Naugle *et al.* [11] did not contain all the relevant values (the two datasets of Silverman fit Eq. 1 perfectly, even if merged together). Yet, it is possible to examine the data by Haviland, Liu and Goldman, in which the quantum phase transition was reported [12]. It should be noted that the exponent is very close to unity ($B = \sim 1$) for the data reported by both Silverman [9,10] and Haviland, Liu and Goldman [12], suggesting that the datasets are also fit well by $\rho T_c = \text{constant}$.

2.1. Bismuth- extracted from Haviland, Liu and Goldman [12] (● in Fig. 4).

Haviland, Liu and Goldman found that the quantum superconducting-insulator transition in their Bi films is around $6.5 \text{ k}\Omega/\square$. This allowed them to report on superconducting films up to $< \sim 5 \text{ k}\Omega/\square$. Since the error in data extraction increased for $d < 0.85$ nm, only data points with $d > 0.85$ nm were considered to examine our model. It should be noted that in the thinnest films, superconductivity may have been influenced by the proximitization with the Ge substrate, hence

changing the trend from a power law to a more complex form. For a more thorough discussion about these thin bismuth films, please see Section 17.2.

Table S2.1. Superconductivity in bismuth films (Haviland, Liu and Goldman [12]), ● in Fig.

4. d , T_c , and R_s reproduced from Fig. 2 and Fig. 3 of Haviland *et al.* [12]. The error in the values extracted for T_c in the two figures is presented as an indication of the data collection error. The values calculated for A , B , T_{c_RC} , and Error in $T_{c_RC}\%$ are also presented.

Taken from Fig. 1 d [nm]	Taken from Fig. 1 T_c [K]	Taken from Fig. 3 $R_s@14K$ [Ω/\square]	Taken from Fig. 3 T_c [K]	Err $T_c\%$	T_{c_RC} [K]	Err $T_{c_RC}\%$
7.407	5.67					
6.41	5.61	154.468	5.614	-0.02	5.19	-7.53
5.376	5.53	168.837	5.521	0.07	5.64	2.08
4.405	5.40	204.76	5.399	0.07	5.63	4.2
3.773	5.29	237.09	5.28	0.12	5.64	6.69
3.322	5.15	294.567	5.1438	0.11	5.11	-0.75
2.95	5.02	330.489	5.016	0.05	5.1	1.62
2.703	4.91	387.966	4.905	0.05	4.71	-4.01
2.519	4.83	402.335	4.825	0.1	4.87	0.83
2.326	4.68	438.258	4.677	0.03	4.82	3.02
2.11	4.53	495.734	4.534	-0.03	4.67	3.02
1.992	4.39	560.395	4.397	-0.04	4.35	-1.02
1.901	4.29	596.318	4.288	0.07	4.27	-0.5
1.757	4.16	668.163	4.153	0.06	4.11	-1.11
1.704	4.09	711.271	4.087	0.12	3.97	-2.99
1.605	3.91	772.34	3.91	0.12	3.87	-1.14
1.529	3.84	819.039	3.833	0.11	3.82	-0.46
1.46	3.75	876.515	3.738	0.25	3.72	-0.73
1.408	3.65	933.992	3.643	0.1	3.61	-1
1.357	3.54	1009.43	3.537	0.17	3.46	-2.35
1.316	3.43	1066.906	3.429	0.16	3.37	-1.87
1.258	3.30	1153.121	3.297	0.23	3.25	-1.64
1.218	3.18	1235.743	3.17	0.23	3.12	-1.79
1.163	3.03	1350.696	3.03	0.13	2.98	-1.77
1.124	2.87	1426.134	2.868	0.12	2.91	1.33
1.093	2.79	1544.679	2.787	0.29	2.75	-1.6

A	6402.8
B	1.043

1.067	2.70	1645.263	2.691	0.19	2.64	-2.1
1.045	2.60	1738.662	2.599	0.18	2.54	-2.45
1.009	2.47	1878.761	2.467	-0.04	2.43	-1.45
0.978	2.31	2047.598	2.306	0.26	2.29	-0.94
0.945	2.16	2216.435	2.153	0.25	2.18	1.03
0.922	2.04	2396.049	2.039	0.23	2.06	0.8
0.895	1.92	2593.624	1.915	0.2	1.96	2.14
0.868	1.75	2794.791	1.754	0.02	1.87	6.59
0.845	1.60	3053.435	1.596	0.29		
0.822	1.45	3297.71	1.44	0.63		
0.802	1.32	3545.577	1.312	0.82		
0.786	1.19	3779.075	1.179	0.62		
0.767	1.03	4073.642	1.024	0.6		
0.752	0.90	4343.062	0.892	0.59		
0.74	0.77	4605.299	0.771	0.23		
0.725	0.65	4892.681	0.652	-0.28		

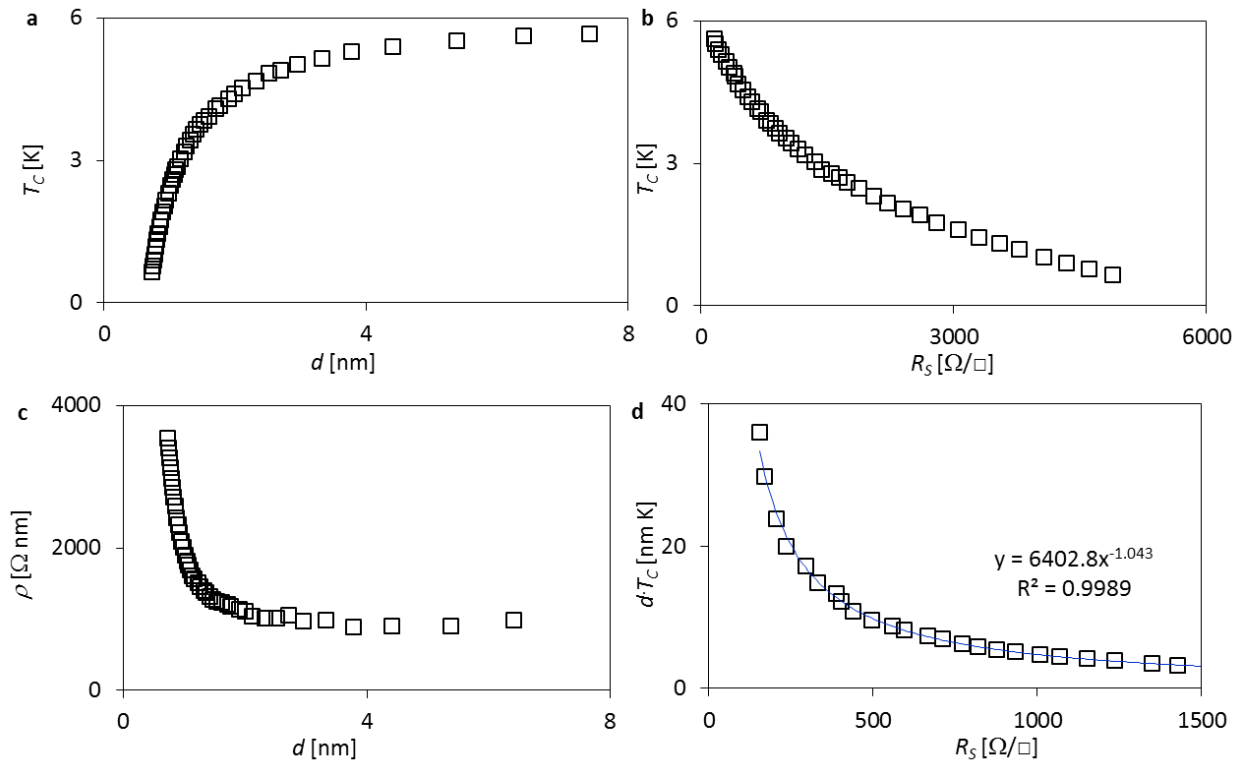


Figure S2.1. Superconductivity in bismuth films (Haviland *et al.* [12]), ● in Fig. 4. Critical temperature as a function of (a) thickness and (b) sheet resistance. (c) Resistivity as a function of thickness. (d) dT_c vs. R_s fits Eq. 1 with $A = 6402.8$ and $B = 1.043$.

3. CoSi₂.

Badoz *et al.* investigated the interplay between conductivity and superconductivity in thin (~1.5 – 70 nm thick) CoSi₂ films [13]. In particular, they were looking at the relation between the deviation from the theory of Fuchs for conductivity in thin metallic films and the suppression of T_c observed in their materials. The authors explained this abrupt change in both superconductivity and metallic behavior with the proximity effect. Unfortunately, we could not extract the data in a way that allows for a reliable examination of the data with Eq. 1, as the mismatch between the extracted data was $\gg 1\%$. Yet, we present below the data we extracted. Yet, Fig. S15 suggests that the data should agree with the found scaling.

Table S3. Superconductivity in CoSi₂ films .

Thickness, R_s and critical temperature values extracted from Badoz *et al.* for CoSi₂ films [13] (Figures 2, inset from 2 and Fig. 3 therein). Large errors in the data extraction process ($\gg 1\%$) do not allow quantitative analysis of the data.

Fig. 2 Inset		Fig2		Fig3		Err $d_{2inset2}\%$	Err $d_{23}\%$	Err $d_{2inset3}\%$
d [nm]	R_s [Ω]	d [nm]	ρ_0/ρ_∞	d [nm]	T_c [K]			
70.922	0.311	60.041	0.94	59.713	1.118	18.122	0.55	18.772
23.095	1.028	20.022	1.112	20.139	1.041	15.347	-0.579	14.679
15.038	2.251	14.166	1.483	14.085	0.928	6.156	0.573	6.764
12.484	2.299	12.092	1.226	12.048	1.013	3.243	0.364	3.619
10.549	3.611	10.1	1.636	10.141	0.852	4.437	-0.396	4.023
				10.121	0.787			
8.203	5.4	7.766	1.961	7.896	0.358	5.634	-1.644	3.898
5.133	12.167	4.644	2.706	4.823	0.22	10.535	-3.713	6.431
4.098	31.679	4.23	4.726			-3.101		
4.08	26.498	4.218	5.314			-3.279		
3.559	31.126	3.546	3.496	3.737	0.02	0.356	-5.101	-4.763
3.549	21.699	3.417	5.029			3.846		
2.535	132.625	2.747	14.826			-7.686		
1.401	1523.5							

4. Ga (from Naugle *et al.* [11] and Ga and In by Jaeger *et al.* [14]).

The data published by Naugle *et al.* [11] on Ga were not sufficiently complete for us to test the scaling of Eq. 1. Moreover, although Jaeger *et al.* [14] reported sets of In and Ga films for granular films (relying in part on Naugle's data), in which the mechanism governing the transition might be considered unusual and different than that of normal films, we wanted to test the scaling of Eq. 1 for these data sets as well. Unfortunately, we encountered technical difficulties in extracting these datasets (the data points are too crowded on the given scales, leading to a large inconsistency error in the extracted data and therefore are not presented here). Yet, we should state here that, although we have low confidence in the data extracted for Ga from Jaeger *et al.* [14], the data we did extract did not fit Eq. 1 very well. However, at this point, we are uncertain whether this disagreement is due to the error in data extraction or due to the fact that the mechanism governing the transition is unique.

5. MgB₂- extracted from Pogrebnyakova *et al.* [15].

Magnesium diboride is often considered a conventional superconductor, even though it is not quite so, due to, *e.g.*, its high transition temperature and the coexistence of two types of Cooper pairs. Moreover, experimental difficulties hinder the understanding of superconductivity in MgB₂. For instance, to date, growing a thin film of high-quality superconducting MgB₂ is still a challenge. In addition, most electrical properties in MgB₂ are anisotropic, which leads to difficulties in obtaining reproducible results. Yet, since MgB₂ is considered a conventional superconductor, we wanted to examine whether the scaling of Eq. 1 can potentially assist in understanding the electronic

properties of this superconductor. To do so, we extracted data for thin films (~80-430 nm thick) of MgB₂ from Pogrebnyakova *et al.* [15].

Since the reported T_c in this dataset spanned a small range (~41-41.8 K), it was impossible to examine the scaling of Eq. 1 quantitatively with respect to its prediction of T_c . Nevertheless, we did find out that the scaling dT_c vs R_s reduces the scattering that exists in other dependencies. Pogrebnyakova *et al.* [15] reported several different datasets of MgB₂ that are distinguishable by their preparation conditions (a flow of B₂H₆ gas with rates ranging from 50 to 250 sccm). Here, we demonstrate the reduction in scattering for one dataset only (200 sccm), in which the effect can be demonstrated qualitatively, but the effect also occurs in most other datasets of this report, though with a lower degree of confidence.

Table S5. Superconductivity in MgB₂ (Pogrebnyakova *et al.* [15]) for 200 sccm B₂H₆ gas flow. d , T_c , and R_s reproduced from Fig. 4 of Pogrebnyakova *et al.* (full squares in the top and bottom panels) [15]. The error in the values extracted for d in the two figures is presented as an indication of the data collection error. The scaling dT_c vs. R_s qualitatively demonstrates a reduction in the data scattering.

Bottom panel		Small panel			Top panel				
d_1	$\rho@14K$	d_2	$\Delta\rho$	Err	d_3 [nm]	T_c	Err	Err	$R_s@300K$
[nm]	[$\mu\Omega$ nm]	[nm]	[$\mu\Omega$ nm]	$d_{12}\%$		[K]	$d_{13}\%$	$d_{23}\%$	[Ω/\square]
80.7	0.84	80.69	9.54	-0.02	80.87	41	0.2	0.22	12.85
151.86	0.37	150.57	8.14	-0.86	151.97	41.3	0.07	0.93	5.61
225.1	0.28	224.4	7.62	-0.31	225.41	41.7	0.14	0.45	3.51
230.08	0.36	229.78	7.92	-0.13	230.83	41.19	0.33	0.46	3.6
337.4	0.6	337.75	11.48	0.1	336.89	41.82	-0.15	-0.25	3.58
364.39	0.33	364.09	9.32	-0.08	363.71	41.42	-0.19	-0.1	2.65
428.41	0.31	428.89	9.59	0.11	428.16	41.47	-0.06	-0.17	2.31

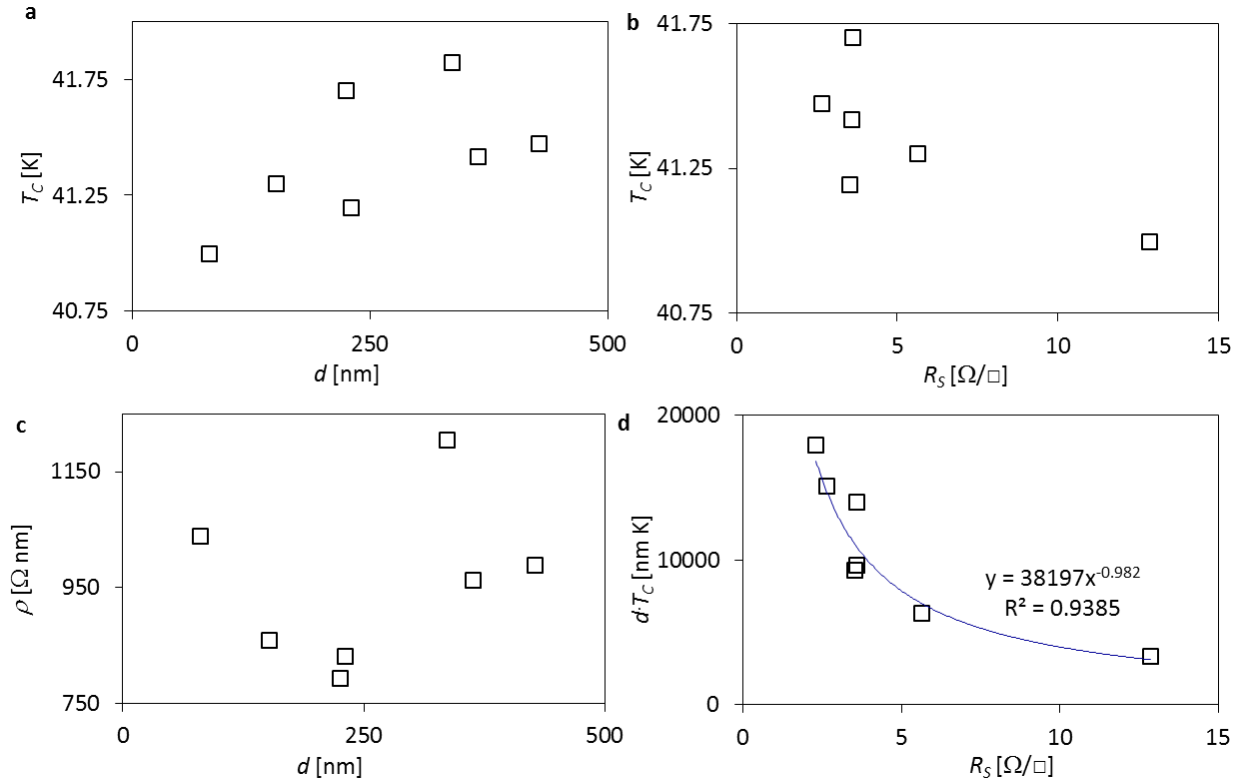


Figure S5.1. Superconductivity in MgB₂ films (Pogrebnyakova *et al.* [15]) for 200 sccm B₂H₆ gas flow. Critical temperature as a function of (a) thickness and (b) sheet resistance. (c) Resistivity as a function of thickness. (d) dT_c vs. R_s demonstrates qualitative agreement with the scaling of Eq. 1, in which the trend is more obvious than in (a-c).

6. Molybdenum (Fàbrega *et al.* [16], [△](#) in Fig. 4).

Similar, *e.g.*, to Al, bulk Mo is a type I superconductor (while thin films of conventional superconductors are effectively type II). The data points presented below were extracted from the work by Fàbrega *et al.* [16], who characterized two-dimensional Mo films. Although these data are in agreement with Eq. 1, the relation between the fitting coefficients A and B do not follow the general trend that seems to appear for the other superconductors examined, as shown in Fig. 5c.

Table S6. Superconductivity in molybdenum films (Fàbrega *et al.* [16]), Δ in Fig. 4. d , T_c , the resistivity at 4.2K and the residual resistivity ratio ($RRR = R_s@300K/R_7@4.2K$) taken from Figures 1 and 3 by Fàbrega *et al.*, [16] as well as the values calculated for A , B , T_{c_RC} , and $Err T_{c_RC}\%$. Since the data points were matched through a common T_c value and through a common thickness value, the difference in T_c and d extracted from the two panels (three datasets) is also added ($Err T_c\%$).

From Fig. 1	From Fig. 1	From Fig. 1	From Fig. 1	From Fig. 3	From Fig. 3	A		99.661	
						B		0.892	
d [nm]	$\rho[\Omega\text{nm}]@4.2\text{K}$	d [nm]	T_c [K]	Err $d\%$	T_c [K]	RRR	Err $T_c\%$	T_{c_RC} [K]	Err $T_{c_RC}\%$
13.252	100.297	13.252	0.707	0	0.709	1.68	0.28	0.777	9.91
16.4	95.21	16.4	0.79	0	0.794	1.74	0.57	0.771	-2.35
21.681	82.493	21.579	0.837	-0.47	0.844	1.82	0.76	0.821	-1.95
28.281	78.847	28.281	0.865	0	0.873	1.879	0.84	0.803	-7.15
41.483	60.958	41.483	0.875	0	0.883	2.089	0.89	0.882	0.81
30.82	64.265	30.922	0.885	0.33	0.894	1.979	1	0.909	2.71
47.576	59.432	47.677	0.888	0.21	0.896	2.1	0.98	0.883	-0.5
52.247	55.108	52.247	0.895	0	0.903	2.149	0.87	0.918	2.54
38.639	62.06	38.639	0.909	0	0.918	2.049	1.03	0.89	-2.05
64.737	56.295	64.737	0.915	0	0.925	2.099	1.08	0.899	-1.81
47.677	66.978	47.677	0.916	0	0.925	1.958	1.05	0.846	-7.57
80.579	50.784	80.68	0.93	0.13	0.94	1.999	1.04	1.004	7.91

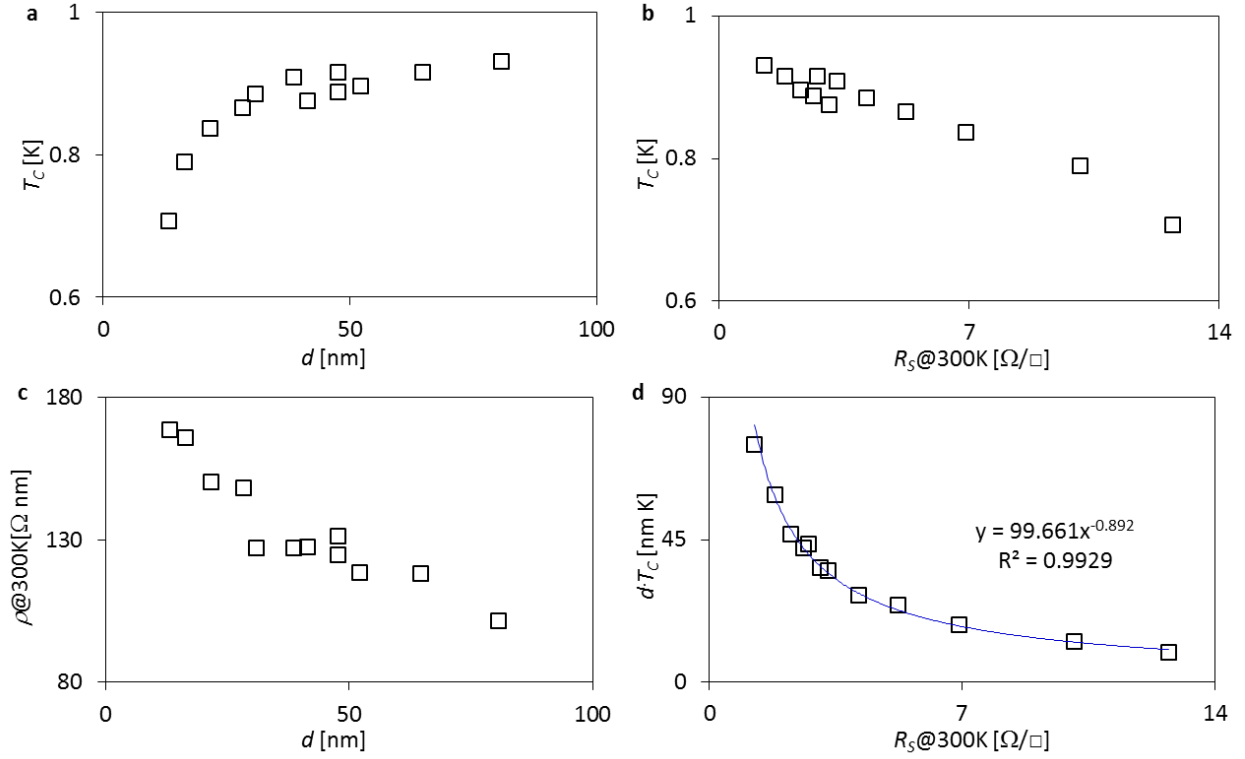


Figure S6. Superconductivity in molybdenum films (Fàbrega *et al.* [16]), \triangle in Fig. 4. Critical temperature as a function of (a) thickness and (b) sheet resistance. (c) Resistivity as a function of thickness. (d) dT_c vs. R_s fits Eq. 1 with $A = 99.661$ and $B = 0.892$.

7. Amorphous MoGe.

The significance of amorphous MoGe films to the understanding of superconductivity has been reported as two-fold by Graybeal and co-authors in 1984 [17], 1985 and in three more occasions, [18–20] as well as by Yazdani and Kapitulnik [21]. First, understanding superconductivity in thin α -MoGe films is interesting from the superconducting-insulator transition perspective. Second, thin α -MoGe films exhibit a deviation from conventional superconductivity that is still not understood. Hence, examining the scaling of Eq. 1 for the case of thin α -MoGe films may address these two issues.

In addition to the importance of these films as was identified by Graybeal and co-author, these films were used to demonstrate the validity of the model for homogeneous superconductors by Finkel'stein [22]. Hence, a comparison of the fitting of the data to the power law presented in this work and to Finkel'stein's model is also brought here, demonstrating that the fitting to Eq. 1 is at least comparable to the fitting of the data to Finkel'stein's model, at least for these films. Moreover, to complete the analysis, we also used these data to examine the universal behavior discussed below in Eq. S2b and we demonstrated that such a universal behavior indeed may exist.

Bearing in mind the universality of Fig. 5a in the main text, α -MoGe is at the extreme where the exponent B (and the coefficient A) has its highest value. Hence, since the other edge of this curve is defined by aluminum, it is possible that the position of a superconductor on this curve is determined by its homogeneity.

Surprisingly, unlike most other materials, the resistivity of several of the data sets of α -MoGe was found to decrease with decreasing thickness. Yet, the α -MoGe data fit Eq. 1 with a very good agreement. Hence, this may strengthen the hypothesis that Eq. 1 encompasses a broader relation between resistance and thickness in metals in general. This may be surprising when bearing in mind that, so far, the electric properties of α -MoGe have been considered as unique and unexplained.

7.1. α -MoGe (Graybeal and Beasley 1984 [17]), in Fig. 4.

Graybeal and Beasley reported the suppression of T_c in thin (> 2 nm) homogeneous films of α -MoGe with reduced thickness [17]. In fact, they reported that the suppression correlates very well the increase in R_s , as suggested by some of the theories at that time that laid the grounds to the later derivation of the dependence of T_c on R_s by Finkel'stein. [22] Yet, as shown below, we found

a very good agreement of the data with the power law of Eq. 1. We should also note that these films were also discussed in a later paper by Graybeal and co-authors [23].

Since this data set is considered a ‘classical’ example for the well-established Finkel’stein’s model, we performed to this data set a somewhat deeper analysis in comparison to the other materials. Specifically, similarly to the analysis done with other materials, in Table S7.1.1 and Fig. S7.1.1 we introduced the analysis of the data with respect to the power law discussed in this work (Eq. 1). However, unlike the analysis done with other materials, here, in Table S7.1.2, we introduced also the values calculated for T_c based on Finkesltein’s model (Eq. 13 in Ref. [22]). For calculating these values that are designated by T_{c_F} we used the values reported for R_s by Graybeal and co-authors as well as $\gamma = -1/8.2$ and $T_{c0}=7.2$ K (γ and T_{c0} correspond to the notation used in Ref. [22]). To allow a visual comparison between the different models, we presented in Fig. S7.1.2 the values of the measured T_c , the re-calculated values for T_c with the fitting to Eq. 1 (T_{c_RC}) and the values for T_c calculated while fitting to Finkel’stein’s model (T_{c_F}) as a function of R_s . Moreover, in Table S7.1.2 we also calculated the error at percent in T_c for each film: $\text{Err } T_{c_F}\% = 100 \cdot (T_{c_F} - T_c) / T_c$. This estimation of the error allows us to quantitatively compare the accuracy of the two models (Finkel’stein’s model and the power law in and Eq. 1) by comparing the errors in the fitting, *i.e.* to compare the value $|\text{Err } T_c\%|$ with the value $|\text{Err}_{T_{c_F}}\%|$ (lower value suggests better accuracy). As shown in both Table S7.1.2 and Fig. S7.1.2 the merit of the fitting of the data of these homogeneous films is at least comparable to the quality of the fit to Finkel’stein’s model for this set of films.

We should remind the reader that presumably, Finkel’stein’s model is used for the correlation between two values that are measured independently (R_s and T_c), while Eq. 1 is using three of such values (R_s , T_c and d). Moreover, presumably, Finkel’stein’s model requires no fitting parameters,

as T_{c0} can, in principle be measured directly and $\gamma=1/\ln(T_{c0}\tau)$ can also be estimated if the relaxation time constant, τ is measured independently. Nevertheless, typically, both T_{c0} and γ are extracted as fitting parameters from the curve $T_c(R_s)$. Likewise, the two parameters A and B in Eq. 1 are also extracted as fitting parameters.

In addition to the comparison to Finkel'stein's model, we used the data of these α -MoGe films to evaluate the fitting of Eq. 1 to the data while using also the possible correlation between the parameters A and B that is introduced below in Eq. S2b. Specifically, it has been proposed that a universal relationship exists between A and B . In such a case, B is the only fitting parameter and is the proportionality factor between $\ln(dT_c/13.7)$ and $\ln(R_s/464)$. Table S7.1.3 presents the fitting value for B with Eq. S2b, as well as the values for the critical temperature that were calculated by feeding back this value of B that was extracted from fitting the data to Eq. S2b as given in Fig. S7.1.3a. We designated these calculated critical temperature values: $T_{c_RC_1Par}$. In Fig. S7.1.3b we compared these values to the values calculated from Eq. 1, to the values calculated with Finkel'stein's model and to the values reported by Graybeal *et al.* as the raw data [23]. Finally, we calculated the error at percent ($ErrT_{c_RC_1Par}\%$) between the value of the re-calculated critical temperature and the measured value as reported by Graybeal *et al.* These values of the error that are presented in Table S7.1.3 demonstrate a reasonable fitting to such a universal behavior (to Eq. S2b). We would like however to remind the reader that despite the agreement of the one-parameter universal description of Eq. S2b with the data here, such a universal approach should describe the data in general and is not necessarily accurate for each of the individual materials. Yet, we should note that although the scatter in Fig. 5a is larger for materials with B close to unity, where the data is more crowded, we do expect the universality of Eq. S2b to describe the materials with B values at the extrema, *i.e.* materials that are relatively more homogeneous or more granular. The α -MoGe

films discussed here are an example for rather homogeneous films. Hence, it is not surprising that their behaviour has a good agreement with Eq. S2b.

Table S7.1.1. Superconductivity in α -MoGe films (Graybeal and Beasley 1984 [17]), \times in Fig. 4.

d , T_c , and R_7 of α -MoGe films of the stoichiometry: 79:21 extracted from Graybeal and Beasley [17]. We present the values calculated for A , B , T_{c_RC} , and Error in $T_{c_RC}\%$ for these films, as well as the error in the data extraction process. One can notice that the three thickest samples had large mismatch between their extracted values, while the thinnest film was reported by the authors to be inhomogeneous (these four films are highlighted in red). Hence, these films were omitted from the calculations.

From Figure 2:		From Figure 1:			A	88643
R_s [Ω/\square]	T_c [K]	R_s [Ω/\square]	d [nm]	Err $R_s\%$	B	1.421
					T_{c_RC} [K]	Err $T_{c_RC}\%$
8.575	7.35	6.901	234.545	-24.254		
		14.374	111.289			
30.088	6.831	29.459	55.321	-2.134		
61.718	6.708	63.993	25.31	3.554		
133.932	6.512	134.685	12.324	0.559	6.833	4.917
165.948	5.994	164.752	10.133	-0.726	6.128	2.233
209.84	5.607	209.822	7.955	-0.009	5.592	-0.258
291.444	5.015	292.471	5.741	0.351	4.858	-3.118
391.014	4.463	391.71	4.391	0.178	4.184	-6.24
472.499	3.992	472.795	3.595	0.063	3.905	-2.192
612.593	3.429	611.156	2.897	-0.235	3.351	-2.266
865.614	2.465	863.818	2.201	-0.208	2.698	9.488
1382.976	1.235	1382.477	1.499	-0.036		

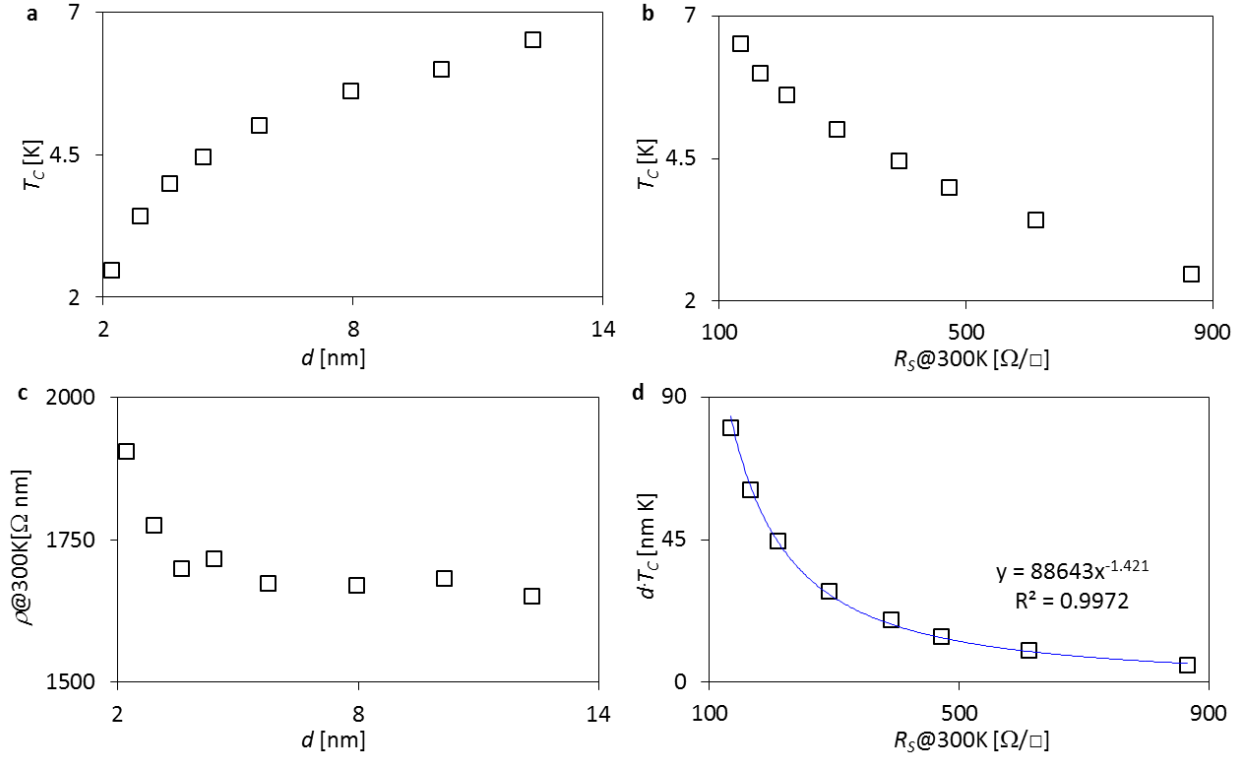


Figure S7.1.1. Superconductivity in α -MoGe films (Graybeal and Beasley [17]), \times in Fig. 4.

Critical temperature as a function of (a) thickness and (b) sheet resistance. (c) Resistivity as a function of thickness. (d) dT_c vs. R_s with a best fit to Eq. 1 with $A = 88643$ and $B = 1.421$.

Table S7.1.2. Comparison of Eq. 1 with the model reported in Ref. [22] for α -MoGe films (Graybeal and Beasley 1984 [17]), \times in Fig. 4.

d , T_c , and R_T of α -MoGe films of the stoichiometry: 79:21 extracted from Graybeal and Beasley [17]. We present a comparison of the discovered scaling law to the analysis of the data with Finkel'stein's model. We calculated the T_c value with Finkel'stein's model (T_{c_F}) by using $T_{c0}=7.2$ K and $\gamma=-1/8.2$, as specified in Ref. [22]. We also presented the error at percent between the fit value for the critical temperature with this model (T_{c_F}) and the actual data that was

extracted from Ref. [17] and we designated this error by: $\text{Err}T_c\text{F}\%$. Therefore, a quantitative comparison between Eq. 1 and the model presented in Ref. [22] can be done by comparing the errors in $\text{Err}T_c\text{RC}\%$ and in $\text{Err}T_c\text{F}\%$

Raw data				Fit to Eq. 1		Fit to Ref. [22]	
R_s [Ω/\square]	d [nm]	T_c [K]	Err $R_s\%$	T_{c_RC} [K]	Err $T_{c_RC}\%$	T_{c_F}	Err $T_{c_F}\%$
8.575	234.545	7.35	-24.254			7.2 K	
	111.289					$\gamma = -1/8.2$	
30.088	55.321	6.831	-2.134				
61.718	25.31	6.708	3.554				
133.932	12.324	6.512	0.559	6.833	4.917	6.316	-3.016
165.948	10.133	5.994	-0.726	6.128	2.233	6.119	2.085
209.84	7.955	5.607	-0.009	5.592	-0.258	5.855	4.43
291.444	5.741	5.015	0.351	4.858	-3.118	5.38	7.282
391.014	4.391	4.463	0.178	4.184	-6.24	4.83	8.234
472.499	3.595	3.992	0.063	3.905	-2.192	4.405	10.335
612.593	2.897	3.429	-0.235	3.351	-2.266	3.723	8.585
865.614	2.201	2.465	-0.208	2.698	9.488	2.652	7.605
1382.976	1.499	1.235	-0.036				

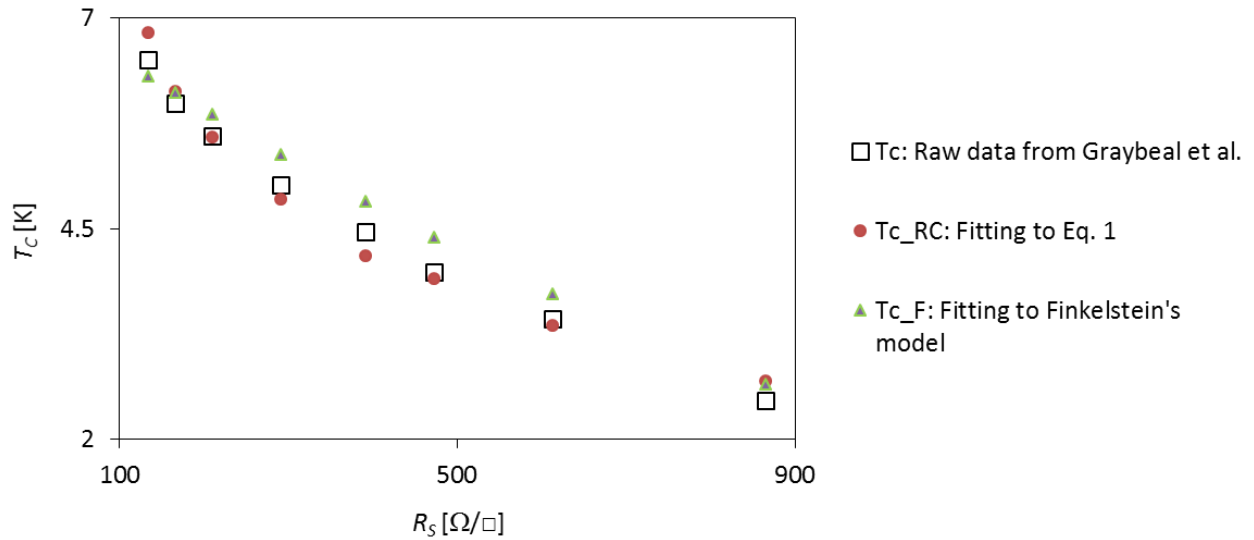


Figure S7.1.2. Comparison between Eq. 1 and Finkel's model for α -MoGe films (Graybeal and Beasley [17]), \times in Fig. 4.

Comparing the power law in Eq. 1 to Finkel'stein's model [22] by presenting the T_c values calculated with each model (*i.e.* T_{c_RC} and T_{c_F} from Table S.7.1.2), as well as the raw data for T_c as was extracted from Graybeal et al. The comparison suggests that the fitting of the data to Eq. 1 is at least comparable to the fitting of the data to the model of Ref. [22].

Table S7.1.3. Fitting the data of α -MoGe films (Graybeal and Beasley 1984 [17], ✗ in Fig. 4) to the one-free-parameter universal formula given in Eq. S2b.

Extracting the value $B=1.5946$ from fitting the proportional terms: $\ln(dT_c/13.7)$ and $\ln(R_s/464)$ as discussed in Eq. S2b and using this value to estimate the values of the critical temperature calculated from this model based on this value of B ($T_{c_RC_1Par}$). The error at percent in the estimated critical temperature is also presented ($ErrT_{c_RC_1Par}\%$), demonstrating a reasonable fitting of the data to the universal behavior of Eq. S2b. Nevertheless, we refer the reader to our remark in the head of this section (S7.1) with regard to the accuracy of this analysis for the general set of data. Red points are omitted from the fitting as explained above.

B= 1.4574		Fit to Eq. S2b	
$\ln(dT_c/13.7)$	$\ln(R_s/464)$	$T_{cRC1Par}$	$ErrT_{cRC1Par}\%$
4.83	-3.99	19.61	166.81
3.32	-2.74	13.35	95.44
2.52	-2.02	10.24	52.65
1.77	-1.24	6.8	4.42
1.49	-1.03	6.05	0.93
1.18	-0.79	5.47	-2.44
0.74	-0.47	4.7	-6.28
0.36	-0.17	4	-10.37
0.05	0.02	3.71	-7.07
-0.32	0.28	3.15	-8.13
-0.93	0.62	2.51	1.84
-2	1.09	1.86	50.63

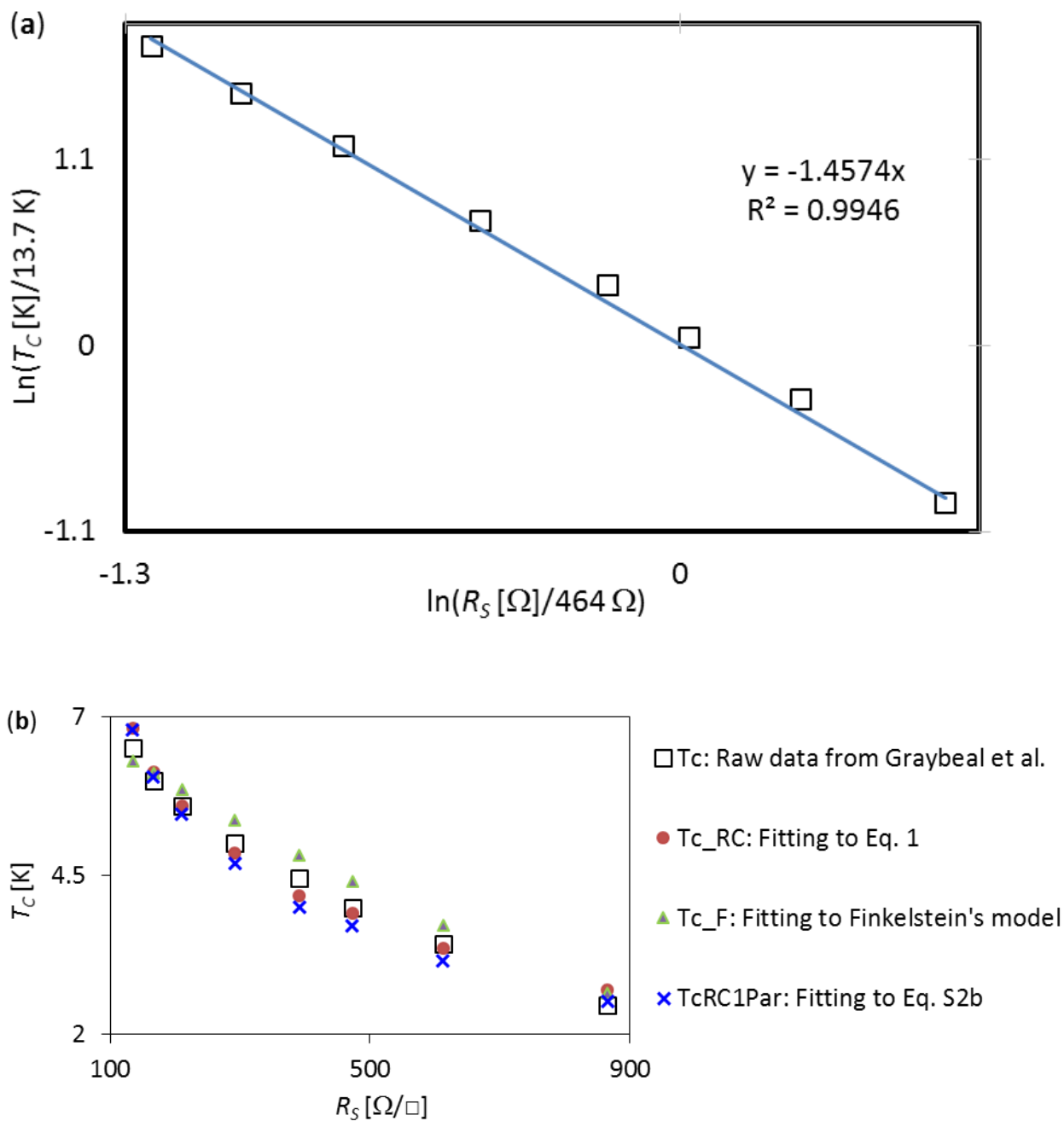


Figure S7.1.3. Analyzing α -MoGe films (Graybeal and Beasley [17], \times in Fig. 4) with the different models.

(a) Extracting B from Eq. S2b from a $\ln(T_c \text{ [K]}/13.7 \text{ K})$ vs. $\ln(R_s \text{ [\Omega]}/464 \text{ }\Omega)$ plot. (b) Comparing the values obtained by the different fittings (Eq. 1, Finkel'stein's model and Eq. S2b, as designated in the legend) to the values reported by Graybeal *et al.*

7.2. α -MoGe (Yazdani and Kapitulnik [21]) (♦ in Fig. 4).

Yazdani and Kapitulnik suggested that the properties of α -MoGe films are sample dependent [21]. They reported two sets of films with different stoichiometries. However, neither of these sets included enough films for our analysis (2 films of α -Mo₂₁Ge and three films of α -Mo₄₃Ge were reported). We combined these two sets, bearing in mind that the scattering may be large. Yet, we found that the data fit Eq. 1 rather well and much better than the other scaling options $T_c(d)$, $T_c(R_s)$ or $\rho(d)$ (Fig. S7.2). It is interesting to note that the values for A and B are consistent with the fact that α -MoGe is at the extreme right of the curve in Fig. 5a. In fact, these values for A and B are also consistent with the linearity in Fig. 5a, strengthening the assumption that A and B are correlated so that each material may be defined by one free parameter only. Finally, we used A and B to calculate the resistance as a function of T_C and d and found the fitting rather valuable (R_{N_RC} in Table S7.1). The error in this re-calculated value for the resistance with respect to the reported resistance (Err R_{N_RC}) is also presented in Table S6.1.

We should note that here, the dependence of T_c and of ρ on film thickness is rather peculiar. We are not sure about the origin of this behavior. However, one possible explanation that can be considered is that the origin of this behavior stems from variations in the film stoichiometry.

Table S7.2. Superconductivity in α -MoGe films from Yazdani and Kapitulnik [21] (♦ in Fig. 4).

d , T_c , and R_s of α -MoGe films with different stoichiometries extracted from Yazdani and Kapitulnik [21]. We also present the values calculated for A , B , T_{c_RC} , and Error in $T_{c_RC}\%$.

				A	2192805		
				B	1.96		
				T_{c_RC}	Err		
	d [nm]	R_N [Ω/\square]	T_c [K]	[K]	$T_{c_RC}\%$	R_{N_RC} [K]	Err $R_{s_RC}\%$
α -Mo21Ge	7	1980	0.1	0.108	8.25	2060.946	4.088
α -Mo21Ge	8	1710	0.15	0.126	-15.83	1566.05	-8.418
α -Mo43Ge	3	1400	0.5	0.498	-0.35	1397.532	-0.176
α -Mo43Ge	4	951	1.01	0.797	-21.04	842.997	-11.357
α -Mo43Ge	6	658	1.02	1.094	7.28	682.025	3.651

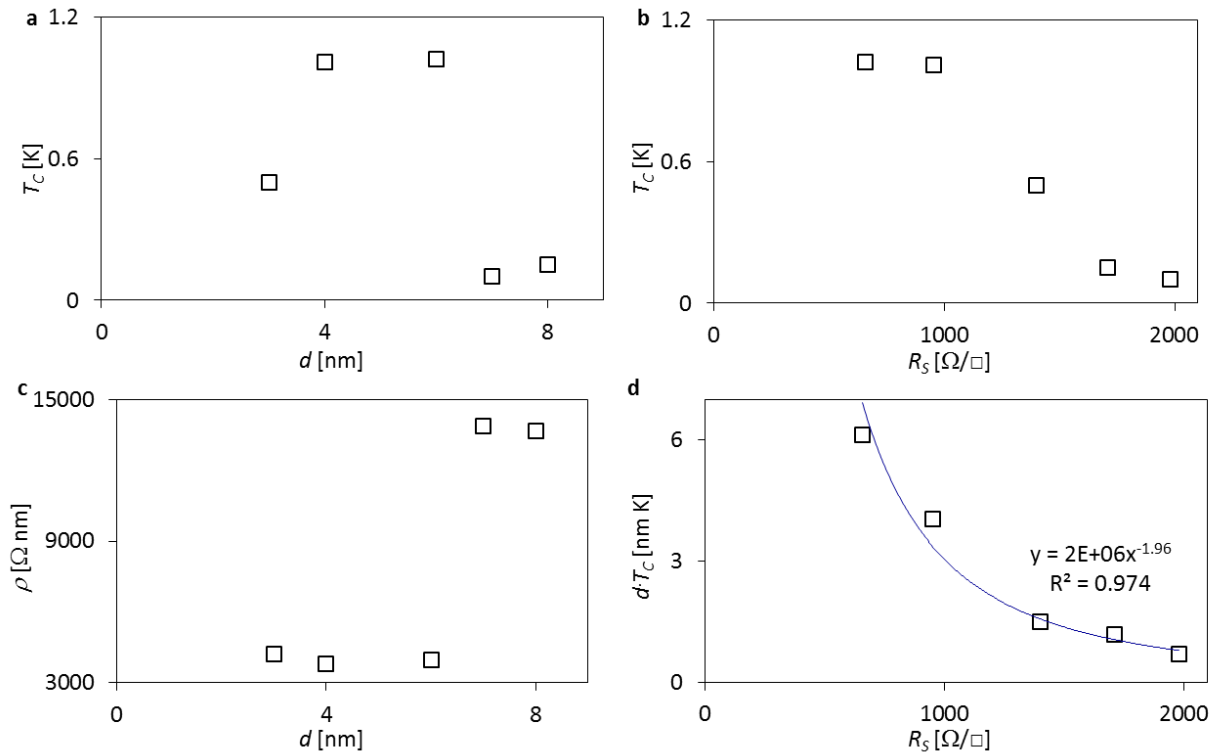


Figure S7.2. Superconductivity in α -MoGe films from Yazdani and Kapitulnik [21] (\blacklozenge in Fig. 4).

Critical temperature as a function of (a) thickness and (b) sheet resistance indicates enhancement of T_c with decreasing thickness. (c) Resistivity as a function of thickness demonstrates a decrease in resistivity with decreasing film thickness. (d) dT_c vs. R_s with a best fit to Eq. 1 with $A = 2192805$ and $B = 1.9601$.

7.3. Amorphous MoGe- extracted from Graybeal and co-authors [18–20] (► in Fig. 4).

Below we present the data for α -MoGe films collected from different reports by Graybeal and co-authors [18–20], which demonstrate excellent agreement with Eq. 1.

Table S7.3. Superconductivity in α -MoGe films (Graybeal and co-authors [18–20]), ► in Fig.

4. d , T_c , and R_s of α -MoGe films extracted from Graybeal and co-authors [18–20] as well as the values calculated for A , B , T_{c_RC} , and Error in $T_{c_RC}\%$. Since the data points were matched through a common T_c value and through a common thickness value, the difference in T_c and d extracted from the two panels (three datasets) are also added (‘Err $T_c\%$ ’ and ‘Err $d\%$ ’). The table includes data merged from the tables in two different publications by Graybeal and co-authors [18,19], while considering their complimentary information [20].

			A	85126
			B	1.389
d [nm]	T_c [K]	R_s [Ω/\square]	T_{c_RC}	Err $T_{c_RC}\%$
6.1	5.442	287	5.379	1.15
4.6	4.92	387	4.709	4.279
2.75	3.734	674	3.645	2.378
2.15	2.999	885	3.194	-6.498
8.3	4.5	260	4.535	-0.78
16.5	6.1	131	5.911	3.092
33	6.9	69	7.2	-4.36

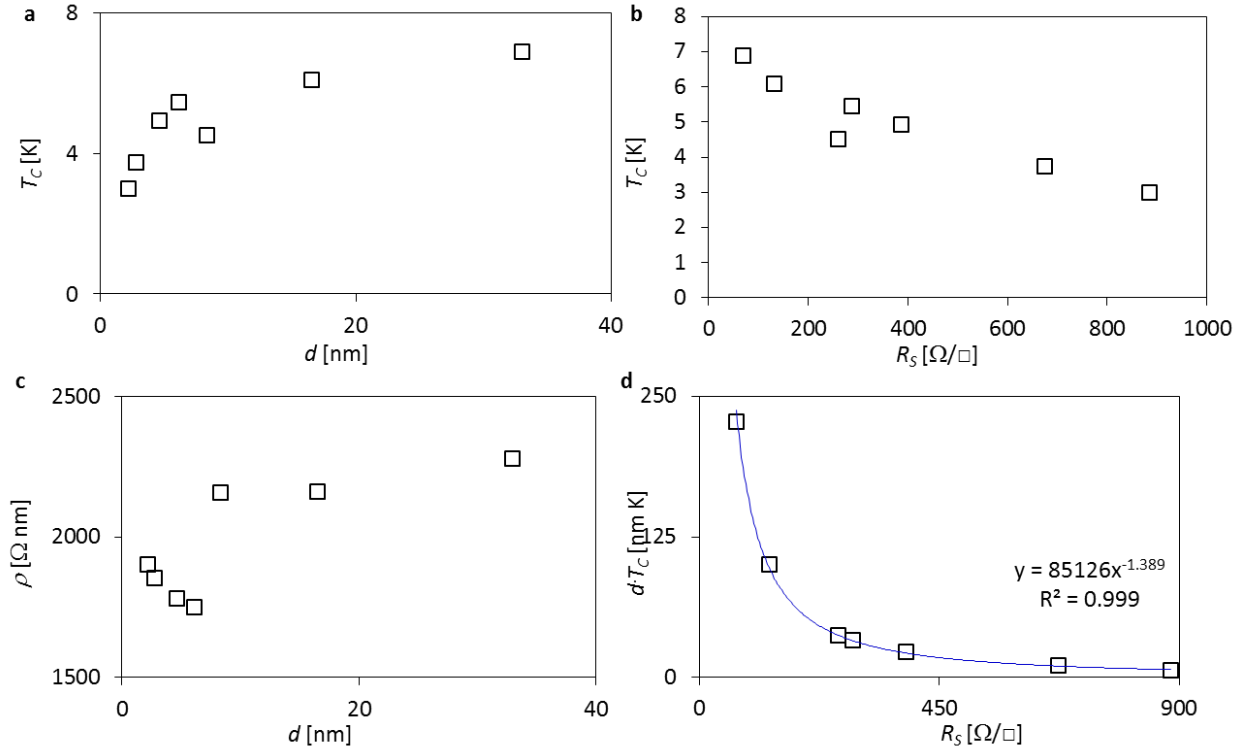


Figure S7.3. Superconductivity in α -MoGe films (Graybeal and co-authors [18–20]), \blacktriangleright in Fig. 4. Critical temperature as a function of (a) thickness and (b) sheet resistance indicates enhancement of T_c with decreasing thickness. (c) Resistivity as a function of thickness demonstrates a decrease in resistivity with decreasing film thickness. (d) dT_c vs. R_s fits Eq. 1 with $A = 85126$ and $B = 1.389$.

8. Nb- extracted from Gubin *et al.* [24] (\blacktriangleleft in Fig. 4).

Gubin *et al.* studied the suppression of superconductivity in thin Nb films on Si substrates with and without the influence of an external magnetic field, suggesting that the mechanism governing superconductivity in these materials is the proximity effect ($T_c = T_c(d)$) [24]. We extracted their data and found that thin Nb films also fit the empirical power law of Eq. 1. However, looking carefully at the data, one can see that, although the error in the fit is low for most of the data points,

it is exceptionally high for one specific data point (highlighted in red in Table S7). Hence, for the sake of data analysis, we fitted the data twice, once with this data point and once without it. This film also varies from the trend when looking at the thickness dependence of the resistivity (Fig. S8c), suggesting that it is different than the other films in this set. The recalculated values were found to be significantly improved when this data point was not considered for the fitting. Here we present the two fitting options in Table S7, while in Fig. S7 we present the fitting curve that included all the data points.

Table S8. Superconductivity in Nb films (Gubin *et al.* [24]), ◀ in Fig. 4. d , T_c , and R_s of Nb films extracted from Gubin *et al.* [24] (Fig. 1 therein) as well as the values calculated for A , B , T_{c_RC} , and Error in $T_{c_RC}\%$. Since the data points were matched through a common a common thickness value, the difference in the extracted d is also added ('Error in $d\%$ '). The data analysis was done with and without the data point highlighted in red, and both calculations are presented.

					With Red Data point		Without Red Data point	
					A	611.38	A	594.13
					B	0.761	B	0.759
					Err			
d [nm]	T_c [K]	d [nm]	R_s [Ω/\square]	Err $d\%$	T_{c_RC}	$T_{c_RC}\%$	T_{c_RC}	Err $T_{c_RC}\%$
7.405	6.134	7.387	29.799	-0.24	6.236	1.67	6.103	-0.52
9.067	6.841	9.173	19.295	1.17	7.089	3.63	6.93	1.31
11.334	7.127	11.28	14.199	-0.47	7.162	0.5	6.997	-1.82
13.148	7.593	13.23	10.397	0.63	7.827	3.08	7.642	0.64
19.646	7.944	18.961	5.925	-3.49	8.035	1.15	7.836	-1.36
49.266	8.802	49.781	2.061	1.04	7.157	-18.69	6.965	-20.87
99.892	9.096	99.774	0.541	-0.12	9.773	7.44	9.485	4.28
199.633	9.477	199.66	0.224	0.01	9.574	1.02	9.276	-2.12
300.13	9.723	300.152	0.124	0.01	9.9835	2.68	9.661	-0.63

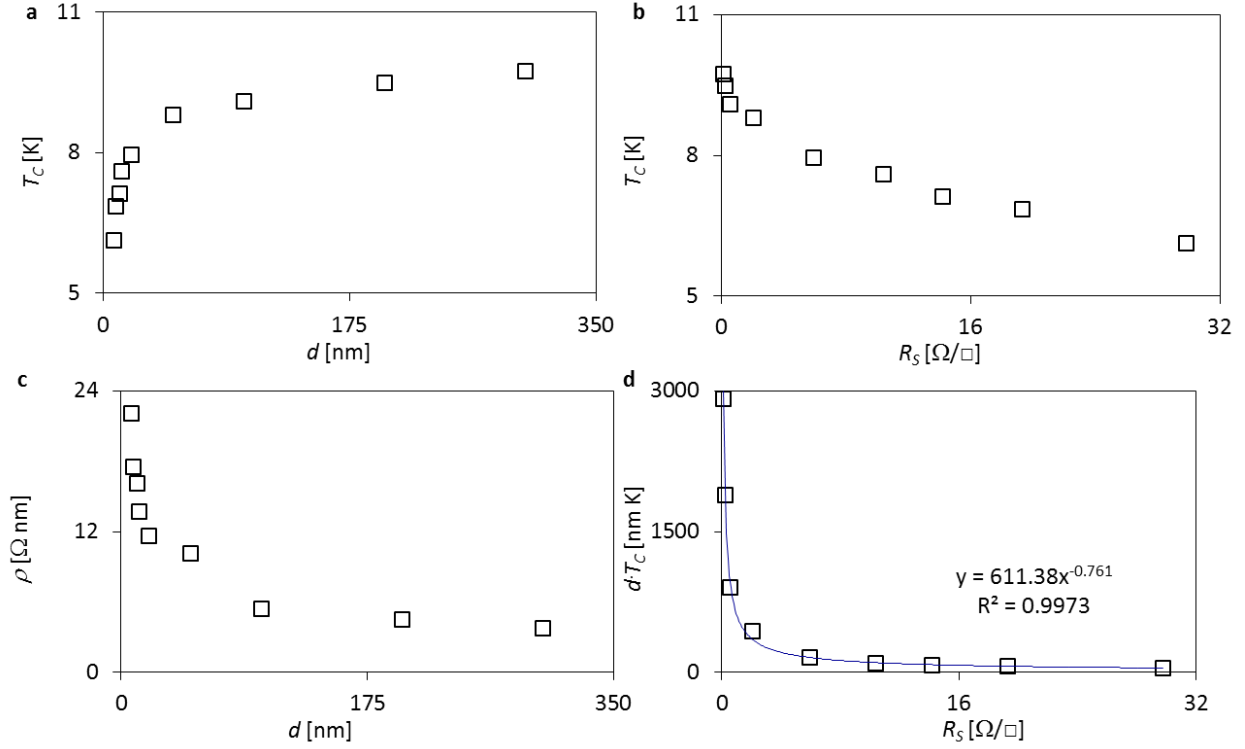


Figure S8. Superconductivity in Nb films (Gubin *et al.* [24]), ◀ in Fig. 4. Critical temperature as a function of (a) thickness and (b) sheet resistance indicates enhancement. (c) Resistivity as a function of thickness. (d) dT_c vs. R_s fits to Eq. 1 with $A = 611.38$ and $B = 0.761$. Data presented in (d) includes the red data point in Table S8.

9. Amorphous Nb₃Ge- extracted from Kes and Tsuei [25] (▶ in Fig. 4).

Kes and Tsuei studied superconductivity in α -Nb₃Ge films [25]. These films cannot be considered thin, as they are ~ 0.5 - $3 \mu\text{m}$ thick. We found that these films scale with dT_c vs. R_s better than they scale, for instance, with $T_c(R_s)$, or with $T_c(d)$ or $\rho(d)$. Nevertheless, we believe that the reason for this is mainly because the changes in T_c for these films are very small (a 10% maximum difference in T_c between the films, which is comparable to the empirical $\pm 5\%$ typical error of the scaling of Eq. 1). Moreover, in these films, R_s is almost inversely proportional to d rather convincingly.

Hence, given the scaling of R_s with d , and given that the exponent B of these films is close to unity, one may wonder whether the origin of the observed scaling in this particular case is mainly due to the electrical properties of the films in the normal state. It should be noted that, in most sets of films with $B = 1$, the scaling of Eq. 1 cannot be explained only with the inverse relations of $R_s(d)$ because the scattering is usually reduced for $dT_c(R_s)$, instead of increasing as it would have been if the reason for this scaling were the inverse relations of $R_s(d)$. In fact, this may still be the case for α -Nb₃Ge, but data for thinner films that enable the examination of the scaling are unavailable to us.

Table S9. Superconductivity in α -Nb₃Ge (Kes and Tsuei [25]), \blacktriangleright in Fig. 4. d , T_c , and R_s of α -Nb₃Ge films extracted from Gubin *et al.* [24] (Fig. 1 therein) as well as the values calculated for A , B , T_{c_RC} , and Error in $T_{c_RC}\%$. Since the data points were matched through a common thickness value, the difference in the extracted d is also added ('Error in $d\%$ ').

			A	6658.3
			B	1.032
d [nm]	T_c [K]	R_s [Ω/\square]	T_{c_RC}	Err $T_{c_RC}\%$
2920	4.25	0.565	4.11	-3.3
1240	3.99	1.266	4.21	5.49
620	3.86	2.645	3.94	1.96
460	4	3.609	3.85	-3.76

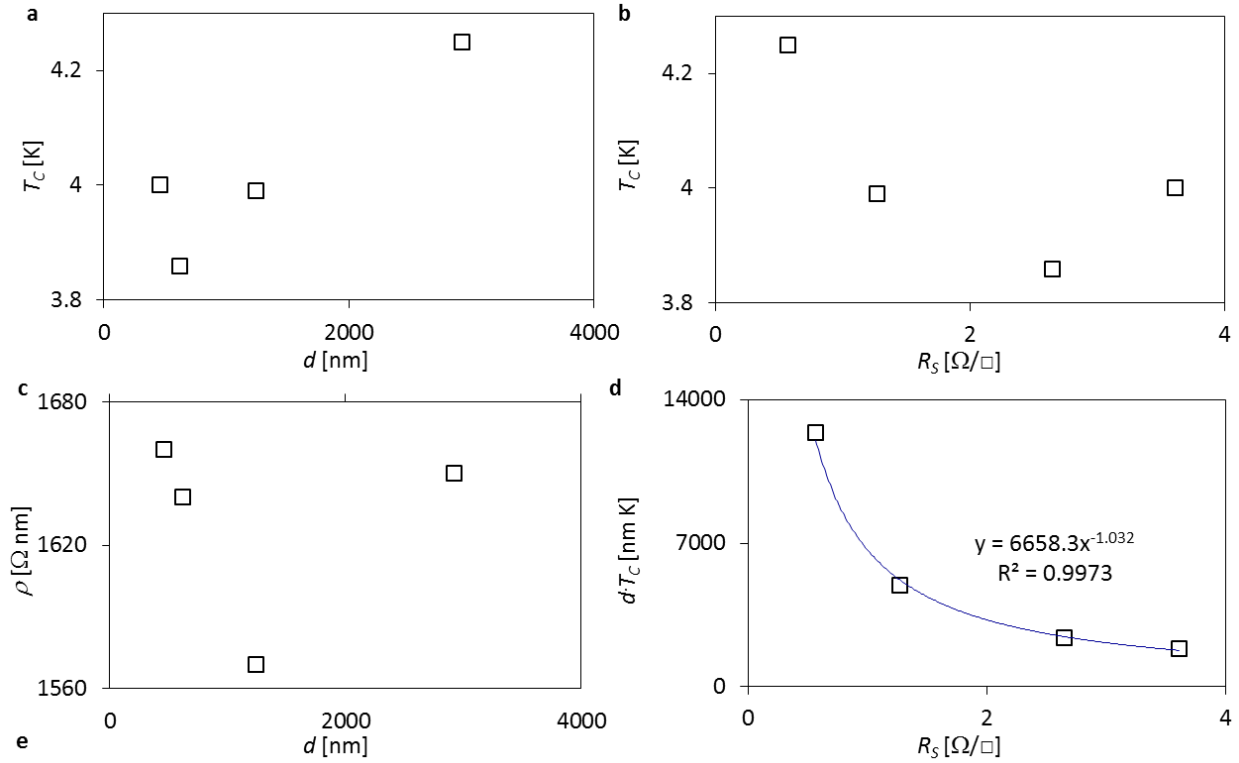


Figure S9. Superconductivity in α -Nb₃Ge (Kes and Tsuei [25]), \blacktriangleright in Fig. 4. Critical temperature as a function of (a) thickness and (b) sheet resistance. (c) Resistivity as a function of thickness demonstrates a decrease in resistivity with decreasing film thickness. (d) dT_c vs. R_s fits to Eq. 1 with $A = 6658.3$ and $B = 1.032$.

10. Nb₃Sn- extracted from Orlando *et al.* [26].

Orlando *et al.* studied superconductivity in what they described as highly damaged or highly defected Nb₃Sn films. This is one of the only examples where the scaling dT_c vs. R_s does not seem to work. We should mention here that, in addition to the defects in the films, the authors also suggested: “since the samples were deposited in a ‘compositional phase spread’ configuration, the unpatterned samples vary to some degree in composition across the films.” [26] In addition, except for one film, all the reported films had a rather constant T_c independent of the thickness, suggesting that they are not in the two-dimensional limit. Lastly, the films were examined over the course of

two calendar years, which may have allowed their degradation. Hence, we do not believe that the fact that these films do not agree with the proposed scaling invalidates it. Yet, we present the data for these films here.

Table S10. Superconductivity in Nb₃Sb (Orlando *et al.* [26]). d , T_c , and R_s of V₃Si films extracted from Orlando *et al.* [26] (Table 1 therein).

d [nm]	R_s [Ω/\square]	T_s [K]
210	0.762	17.9
730	0.121	17.9
260	0.654	17.8
510	0.704	16.1

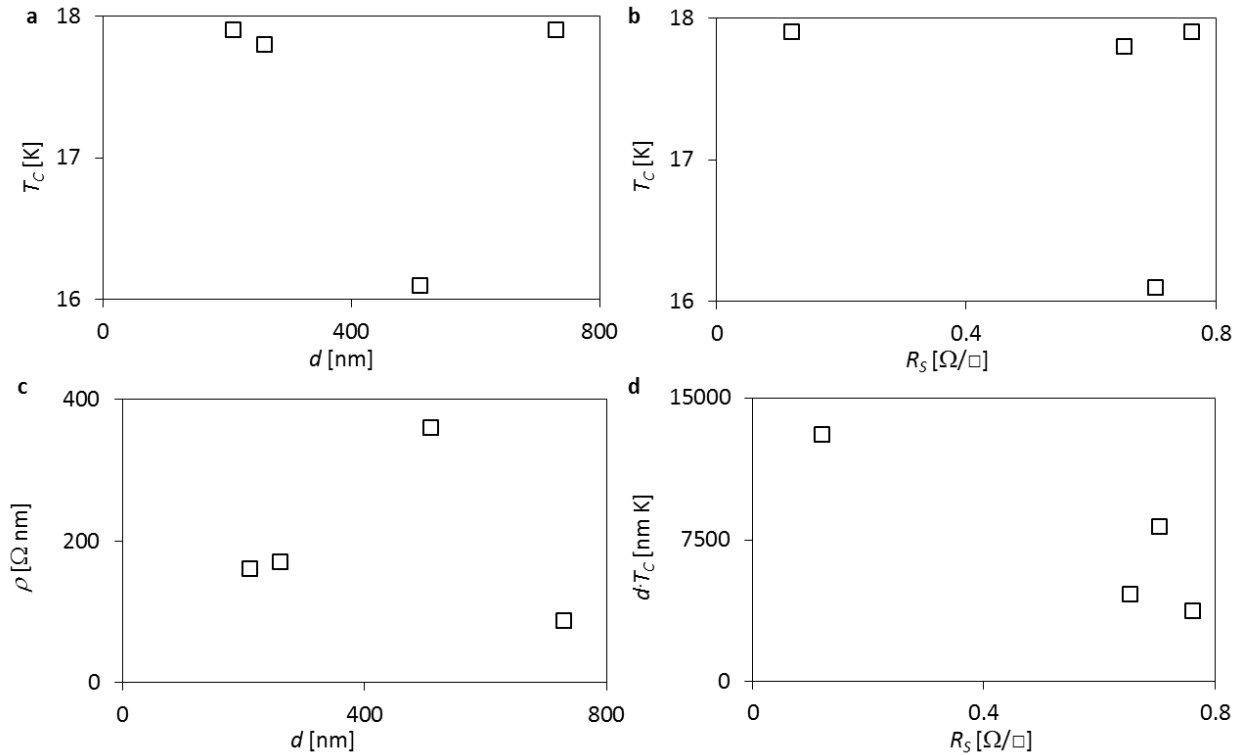


Figure S10. Superconductivity in Nb₃Sn (Orlando *et al.* [26]). Critical temperature as a function of (a) thickness and (b) sheet resistance. (c) Resistivity as a function of thickness. (d) dT_c vs. R_s does not fit the highly-defected and inhomogeneous thick films well.

11. NbN.

As mentioned in the main text, superconductivity in NbN is appealing from both technological and fundamental science perspectives. In addition, each of the following datasets is reported to fit a different scaling. Hence, there is also a need to seek a general mechanism that can describe all these datasets. Although the source of the scaling proposed here and that of the empirical power law of Eq. 1 is unknown, demonstrating universal behavior empirically is essential in the process of seeking a general mechanism.

11.1. NbN- extracted from Wang and co-authors [27–29] (■ in Fig. 4).

We merged data from three different works by Wang and co-workers, in which they grew NbN on MgO substrates [27–29]. In their latest work, the authors found that the suppression of T_c scales with R_s in accordance to Finkel'stein's theory [22]. Indeed, Fig. S11.1b demonstrates a relatively low level of scatter. Yet, we found that these data can also be fitted by Eq. 1 with good agreement.

It should be noted that in two of the samples the error in the extracted values was higher than in the others. The authors also reported lower confidence in the thickness values for the thinner films (highlighted in red in Table S11.1). We included these values and made the fitting with and without them, as well as only for the older report [27], only for the second report [28] and for the first and latter works [27,29]. Moreover, we presented the dT_c vs. R_s curves for these three datasets separately in Fig. S11.1. We should mention here that, although an inverse proportional relation between R_s and d was suggested, this by itself cannot explain the fitting to Eq. 1, with which the data was found to be in better agreement.

Finally, it should be noted that, although the authors reported some of the thickness values explicitly, not all the films were identified, so we extracted them from their figures, as detailed in Table S11.1.

Table S11.1. Superconductivity in NbN (Wang and co-authors [27–29]), ■ in Fig. 4. d , T_c , and R_s of NbN films extracted from Wang and co-authors [27–29] (Fig. 3 in the older reference [27], Fig. 3 in [28] and Fig. 1 and 4 in the newer report [29]) as well as the values calculated for A , B , T_{c_RC} , and Error in $T_{c_RC}\%$. Since the data points were matched through a common critical temperature value, the difference in the extracted T_c in the second dataset is also added (‘Err in $T_c\%$ ’). The data analysis was done with and without the data points for which the authors reported low confidence of their d values by the authors (highlighted in red), as well as due to the data extraction process (highlighted in blue), and both calculations are presented. Older data [27] are separated from newer data [29] by a horizontal line, while the report from 2002 [28] is brought below the data points, in the end of the table.

d [nm]	T_c [K]	$R_s@20K$ [Ω/\square]	T_c [K]	Err $T_c\%$	With red values		Without red values		Older paper	
					Old and New		Old and New		only [27]	
					[27,29]		[27,29]		[27]	
					A	12141	A	10471	A	10843
					B	1.041	B	0.9935	B	0.984
					T_{c_RC} [K]	Err $T_c\%$	T_{c_RC} [K]	Err $T_c\%$	T_{c_RC} [K]	Err $T_c\%$
5	12.5	174			11.29	-9.68	12.45	-0.4	13.54	8.32
9	14	95.556			11.71	-16.36	12.54	-10.43	13.56	-3.14
17	14.5	50			12.17	-16.07	12.64	-12.83	13.58	-6.34
40	15.5	18.75			14.35	-7.42	14.23	-8.19	15.15	-2.26
85	15.5	8.412			15.56	0.39	14.85	-4.19	15.69	1.23
175	15.6	4			16.39	5.06	15.09	-3.27	15.84	1.54
340	15.9	2.03			17.09	7.48	15.25	-4.09	15.89	-0.06
700	16	0.957			18.15	13.44	15.62	-2.38	16.17	1.06
19.76	14.48	34.3	14.486	0.04	15.5	7.04	15.81	9.19		
12.39	14.013	70.3	14.044	0.22	11.71	-16.43	12.36	-11.8		
12.9	13.712	42.4	13.741	0.21	19.04	38.86	19.62	43.09		
9.91	13.566	78.5	13.551	-0.13	13.05	-3.83	13.85	2.07		
7.43	13.126	103.1	13.135	0.06	13.11	-0.12	14.09	7.34		
5.17	11.107	250.5	11.089	-0.17	7.47	-32.75	8.38	-24.55		
3.98	10.545	258.6	10.572	0.25	9.39	-10.96	10.55	0.04		
2.5	7.822	597.9	7.868	0.59	6.25	-20.1	7.3	-6.67		
2.6	3.689	1056.8	3.699	0.27	3.32	-10.01	3.99	8.15		

1.99	2.676	1035.4	2.665	-0.42	4.43	65.55	5.32	98.81
1.99	2.51	1189.6	2.562	2.09	3.84	53.01	4.63	84.49

d [nm]	T_c [K]	$R_s@20K$ [Ω/\square]	d [K]	Err d %	All data [27–29]		All but red points		From $T_c(d)$ [28]		From $\rho(d)$ [28]	
					A	B	A	B	A	B	A	B
					11275	1.006	9465.4	0.946	7693.9	0.889	7908.7	0.891
					T_{c_RC} [K]	Err T_c %	T_{c_RC} [K]	Err T_c %	T_{c_RC} [K]	Err T_c %	T_{c_RC} [K]	Err T_c %
2.866	9.74	639.875	2.814	1.848	5.914	39.283	7.316	24.89	8.595	11.763	8.882	8.809
4.314	12.271	267.95	4.255	1.399	9.432	23.135	11.074	9.752	12.38	-0.889	12.76	-3.987
5.784	12.69	212.665	5.665	2.095	8.877	30.051	10.278	19.004	11.34	10.639	11.774	7.219
7.213	13.417	140.63	7.1	1.589	10.79	19.577	12.188	9.158	13.133	2.111	13.58	-1.215
10.106	14.352	81.696	9.941	-1.66	13.3	7.33	14.542	-1.319	15.192	-5.851	15.736	-9.642
14.416	14.524	55.868	14.23	1.308	13.666	5.912	14.604	-0.551	14.93	-2.798	15.423	-6.192
21.651	14.914	35.165	21.386	1.241	14.496	2.804	15.067	-1.027	15.002	-0.595	15.502	-3.943
28.902	15.085	25.181	28.561	1.196	15.195	-0.73	15.48	-2.623	15.124	-0.257	15.631	-3.618
86.909	15.727	7.547	85.77	1.328	16.982	-7.983	16.095	-2.34	14.68	6.656	15.229	3.1678
174.02	15.777	3.593	172.66	0.789	17.895	13.425	16.221	-2.815	14.182	10.1	14.656	7.106

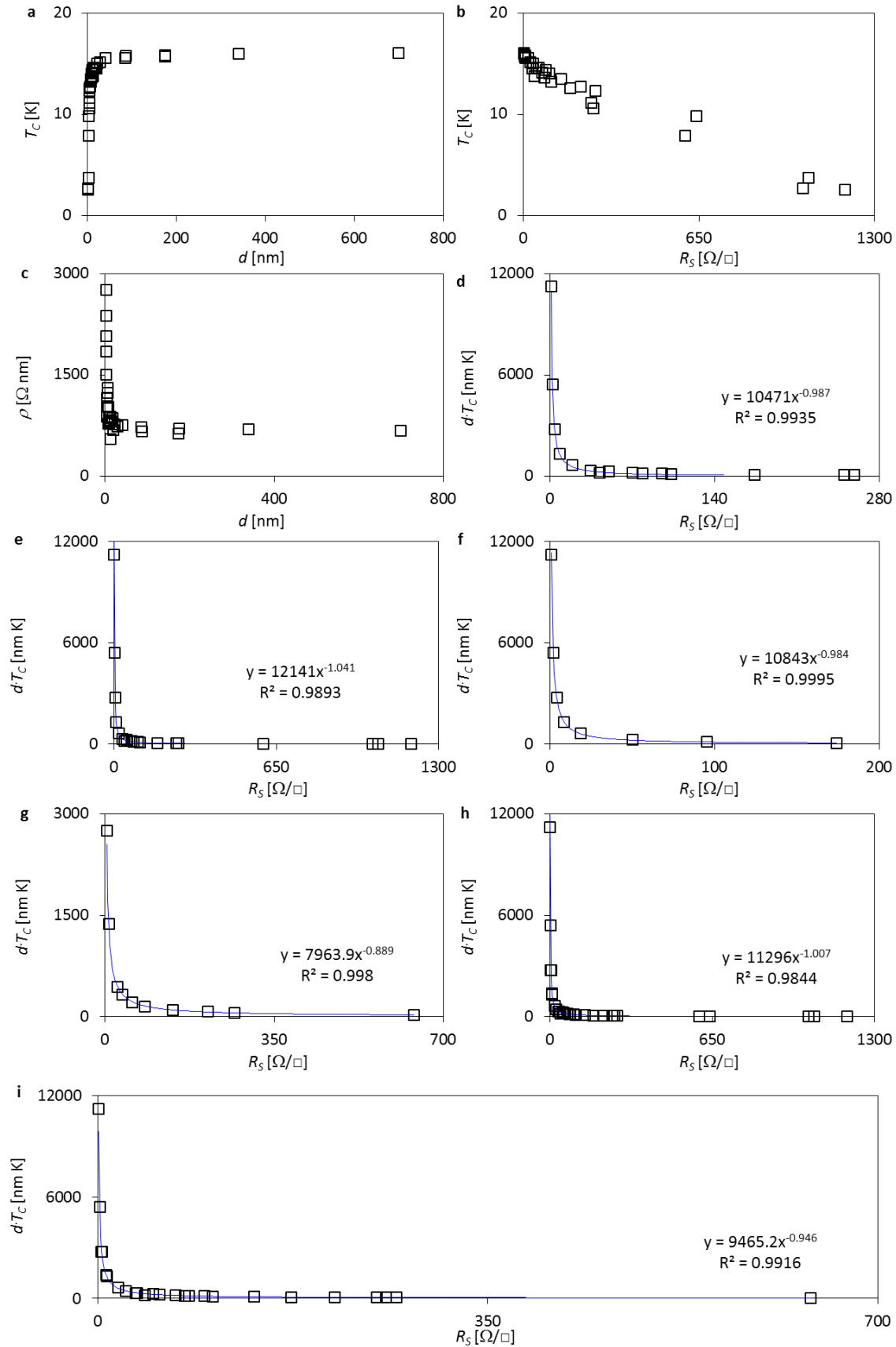


Figure S11.1. Superconductivity in NbN (Wang and co-authors [27–29]), ■ in Fig. 4. Merged data from Wang *et al.* [27,29] for critical temperature as a function of (a) thickness and (b) sheet resistance. (c) Resistivity as a function of thickness. (d) dT_c vs. R_s from these merge data without data points that had a lower level of certainty in their thickness values (highlighted in red in Table S10.1). (e) dT_c vs. R_s for all the data presented in Table S10.1. (f) dT_c vs. R_s from one dataset only (the older paper by Wang *et al.* [27]). (g) dT_c vs. R_s for data only from the 2000 report [28]. (h) dT_c vs. R_s for all the three data sets [27–29]. (i) dT_c vs. R_s for all the three data sets [27–29], not including the data points marked in red in Table S11.1.

11.2. NbN- extracted from Semenov *et al.* [30] (■ in Fig. 4).

Semenov *et al.* optimized the conditions for growing NbN films on sapphire while maximizing T_c at the different thicknesses. In addition to variations in growth conditions, some films were of different physical dimensions in the x-y plane. Semenov *et al.* reported good agreement of their data with the proximity effect model, so they found that T_c is a function of d . Moreover, they presented two data points for NbN films that were grown with nitrogen deficiency and hence were chemically, crystallography and electronically different than the other superconducting films in this dataset.

We present these films in Table S11.2 and Fig. S11.2 (we included the films of all physical dimensions but took only the large continuous films into consideration in the calculations). One can appreciate that these films fit the empirical power law of Eq. 1 well. Moreover, the films that were grown with nitrogen deficiency were clearly distinguishable from the others (highlighted in red in Table S11.2). This observation strengthens the fact that the scaling of Eq. 1 can be used for

controlling and studying the quality of superconducting films, a fact that is significant both experimentally and technologically.

Table S11.2. Superconductivity in NbN (Semenov *et al.* [30]) ■ in Fig. 4. d , T_c , and R_s of NbN films extracted from Semenov *et al.* [30] (Tables 1 and 3 therein) as well as the values calculated for A , B , T_{c_RC} , and Error in $T_{c_RC}\%$. Films highlighted in red were reported to be grown with nitrogen deficiency, while values highlighted in blue are of films with varying geometries and hence are different than the others.

d [nm]	T_c [K]	$R_s@295K$ [Ω/\square]	A	9544.2
			B	0.854
			T_{c_RC} [K]	Err $T_c\%$
3.2	9.87	707	10.99	11.4
3.3	10.84	688	10.91	0.67
3.9	11.84	572	10.81	-8.69
4.3	12.44	478	11.43	-8.12
5.1	13.23	341	12.86	-2.81
5.6	12.99	280	13.86	6.68
5.8	13.5	265	14.02	3.88
8	13.99	191	13.45	-3.88
8.3	14.4	165	14.69	1.99
11.7	15.2	105	15.33	0.84
14.4	15.25	84	15.07	-1.2
5.3	11.54	261	15.55	34.73
6.7	13.47	145	20.32	50.83
3.2	10.72	940.62	8.62	-19.63
6	14.02	235	15.02	7.14
12	15.17	90.83	16.91	11.49

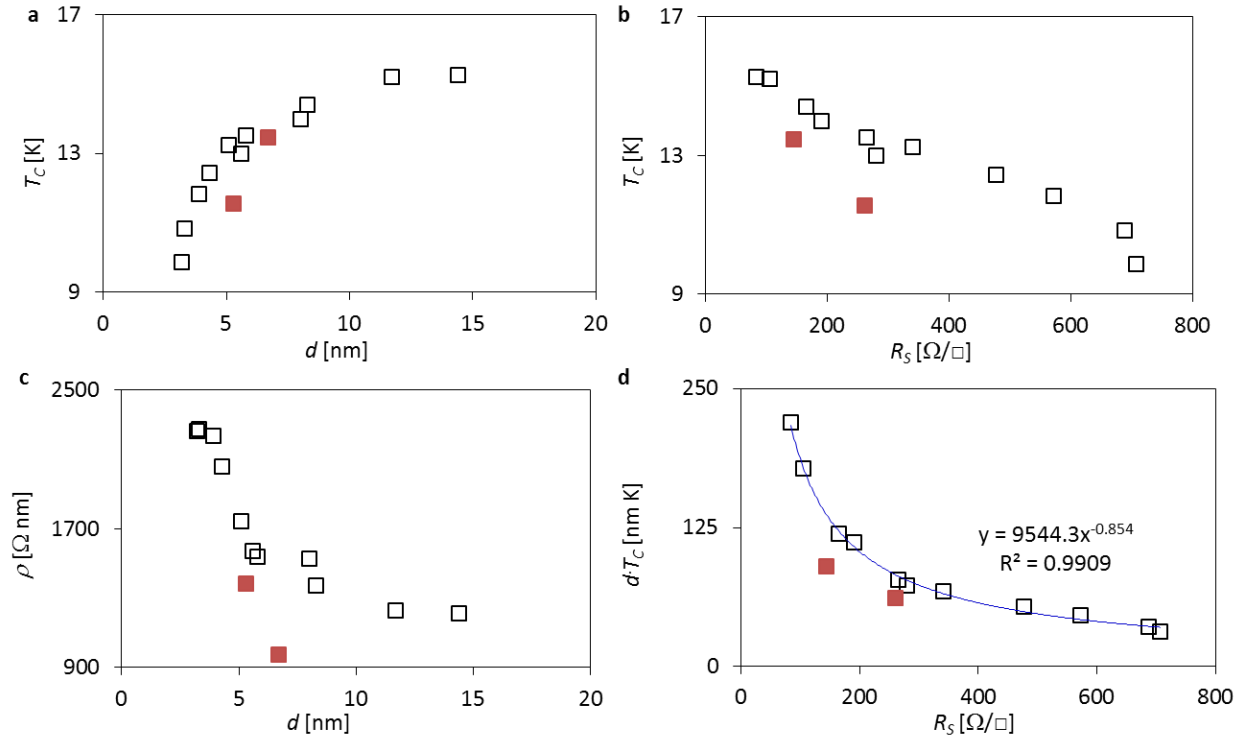


Figure S11.2. Superconductivity in NbN (Semenov *et al.* [30]) ■ in Fig. 4. Critical temperature as a function of (a) thickness and (b) sheet resistance. (c) Resistivity as a function of thickness. (d) dT_c vs. R_s for all films that were prepared under ‘normal’ conditions (not highlighted in red in Table S11.2). Red data points were reported by Semenov *et al.* to be grown with nitrogen deficiency. These films are not considered for the fitting, but their distance from the trend line in (d) and high values in $\text{Err } T_{c_RC}\%$ suggest such films can be distinguished when plotting dT_c vs. R_s . $A = 9544.2$, $B = 0.854$.

10.3. NbN (Kang *et al.* [31], □ in Fig. 4).

Kang *et al.* supplied a review of some prior works on NbN films. They suggested that, for these films, T_c scales with thickness in accordance with the quantum size effect model ($T_c = T_c(d)$). Moreover, they suggested that the electrical properties of the films change at $d = \sim 5$ nm [31]. We found that their data (extracted from Figures 3 and 4, as well as directly from the authors) fit Eq.

1 but not with a great accuracy. A possible reason for that is the reported large error bars in thickness values, mainly for the thinner films.

Table S11.3. Superconductivity in NbN (Kang *et al.* [31]) \square in Fig. 4. d , T_c , and R_s of NbN films extracted from Kang *et al.* [31] (Figures 3 and 4 as well as data that were sent directly by the authors) as well as the values calculated for A , B , T_{c_RC} , and Error in $T_{c_RC}\%$.

d [nm]	T_c [K]	R_s [Ω/\square]	T_{c_RC} [K]	Err $T_c\%$
3.3	11	498.435	10.42	-5.3
4	11.8	399.431	10.36	-12.16
5	13.2	184.642	15.93	20.66
7	14.1	125.353	15.79	11.97
9	14.5	98.8	15.02	3.58
13	15	67.784	14.3	-4.66
20	15.4	42.964	13.67	-11.23

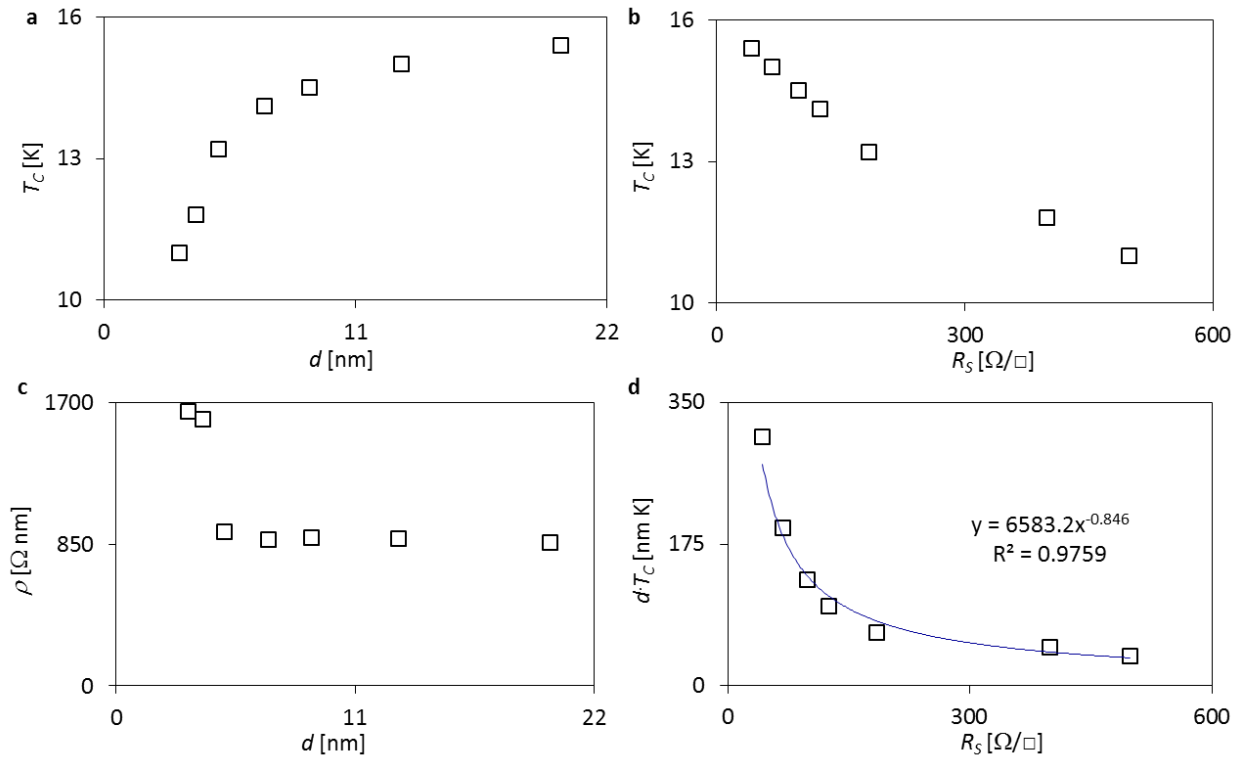


Figure S11.3. Superconductivity in NbN films (Kang *et al.* [31]) \square in Fig. 4. Critical

temperature as a function of (a) thickness and (b) sheet resistance. (c) Resistivity as a function of thickness. (d) dT_c vs. R_s . $A = 6583.2$, $B = 0.846$.

11.4 NbN (Delacour *et al.*) [32].

Delacour *et al.* reported and analyzed superconducting NbN films deposited on sapphire. However, since the data of the reported films that are distributed over a relatively narrow thickness range is scattered over three different graphs (Fig. 5b, Fig. 7 and Fig. 8 in Reference [32]), we could find complete data (d , T_c and R_s) for only three films. Moreover, the values of these three films are rather close, decreasing the reliability of an analysis with respect to Eq. 1 (*e.g.*, the scale for d is 3-5 nm, while it is 4.4-6.4 K for T_c). Hence, we did not have high enough confidence to add these values to Fig. 2. Yet, we present here the relevant data (Table S11.4) and graphs (Fig. S11.4).

Table 11.4. Superconductivity in NbN (Delacour *et al.* [32]).

d , T_c , $R_s@10K$, the residual resistance ratio (RRR), and the values of the errors in the extraction process of NbN films extracted from Delacour *et al.* [32] Values for which a match was found are highlighted.

From Fig. 7		From Fig. 8		From Fig. 5b					
$R_s@10K$ [Ω/\square]	T_c [K]	T_c [K]	d [nm]	d [nm]		RRR ⁻¹	$R_s@300K$ [Ω/\square]	Err $T_{c7,8}\%$	Err $d_{5b-8}\%$
		9.203	199.084	202.072		0.028			1.501
		9.092	98.629	100.455		0.031			1.851
		7.588	8.84	8.925		0.414			0.958
		6.608	6.492	6.523		0.775			0.49
225.836	6.91								
246.466	6.403	6.509	4.993	5.035		0.926	228.105	1.656	0.835
		6.2	4.018						
347.184	4.901	5.005	3.344	3.344		3.233	1122.375	2.109	0.01
497.513	4.411	4.5	2.982	2.986		4.344	2160.997	2.051	0.141
				2.81		12.588			

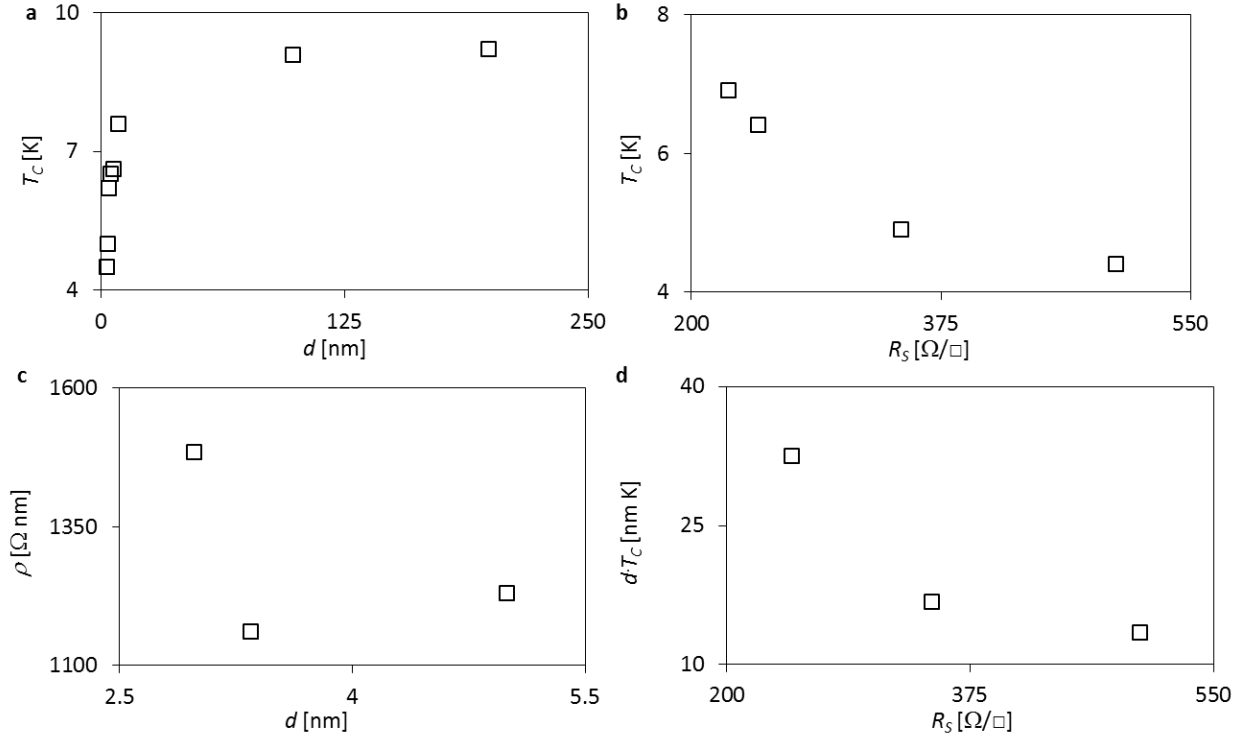


Figure S11.4. Superconductivity in NbN films (Delacour *et al.* [28]). Critical temperature as a function of (a) thickness and (b) sheet resistance. (c) Resistivity as a function of thickness. (d) dT_c vs. R_s . The small number of points in (d) does not allow a quantitative fit to Eq. 1.

11.5. NbN- Our films (○ in Fig. 4).

The relations between the different values for the 32 NbN films grown by us were presented in the main text. Here we detail the exact values of the films. The agreement of our films with Eq. 1 was discussed broadly in the main text. The data presented here also include the two films (highlighted in red) whose substrates came into contact with water prior to deposition, which is suspected of influencing their properties (MgO reacts aggressively with water). We found that the best scaling that fits our data is dT_c vs. R_s , but we also present the best fit to the power law of Eq. 1.

Table S11.5. Superconductivity in our NbN films, ○ in Fig. 4. d , T_c , and R_s of NbN films grown and characterized by us on MgO substrates as well as the values calculated for A , B , T_{c_RC} , and

Error in $T_{c_RC}\%$. Data include two films where chemical treatment of the substrate prior to deposition is suspected of influencing their properties (highlighted in red).

			A	9448.1
			B	0.903
d [nm]	R_s [Ω/\square]	T_c [K]	T_{c_RC} [K]	Err $T_{c_RC}\%$
5.67	294.53	10.7	9.82	-8.22
5.46	303.96	10.9	9.91	-9.06
5.43	301.60	10.7	10.04	-6.19
5.43	297.39	11.3	10.17	-10.04
5.2	275.31	11.5	11.38	-1.04
5.32	271.10	11.7	11.28	-3.59
5.18	252.99	11.5	12.33	6.81
5.27	259.07	11.6	11.86	2.58
6.2	337.20	8.3	7.95	-4.24
2.88	600.79	9.9	10.16	2.6
3.18	396.08	11.0	13.4	21.82
4.3	369.80	10.6	10.54	-0.53
5.7	311.51	9.6	9.29	-3.26
5.4	316.27	9.8	9.67	-1.33
5.4	177.46	14.2	16.29	14.74
5.7	204.23	13.5	13.6	0.72
5.9	274.29	11.3	10.06	-10.93
5.8	275.00	11.3	10.21	-9.61
6.5	318.65	8.7	7.98	-8.29
6.4	321.03	8.7	8.05	-7.48
5.5	292.72	11.5	10.18	-11.47
6.2	188.41	13.2	13.44	1.85
4.4	297.84	12.0	12.53	4.4
3.5	396.44	11.4	12.17	6.71
16	54.12	15.1	16.07	6.42
7.9	146.90	13.4	13.21	-1.42
9.3	103.60	14.5	15.38	6.08
6.3	206.96	12.7	12.16	-4.29
3.6	450.01	9.2	10.55	14.65
2.9	542.30	9.5	11.06	16.47
6.4	430.70	13.3	6.17	-53.59
6.5	494.21	10.5	5.37	-48.87

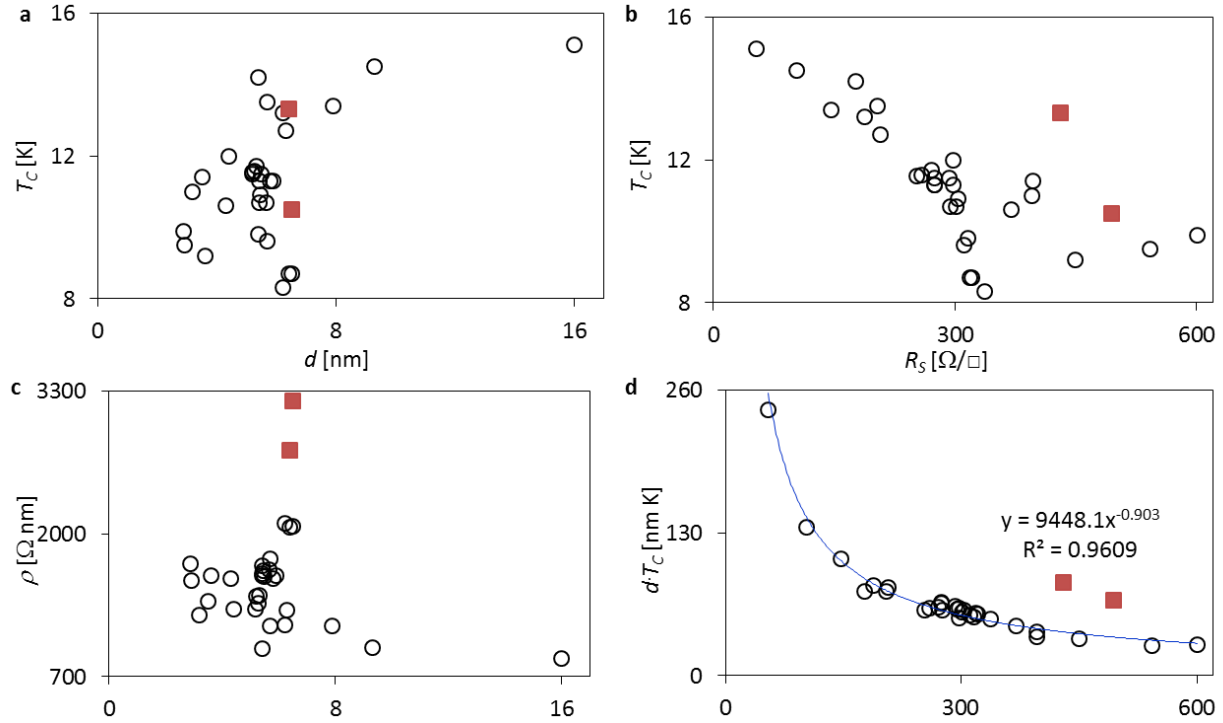


Figure S11.5. Superconductivity in our NbN films, \circ in Fig. 4. Critical temperature as a function of (a) thickness and (b) sheet resistance. (c) Resistivity as a function of thickness. (d) dT_c vs. R_s . Chemical treatment of the substrate prior to deposition is suspected of influencing the properties of the films presented here as red squares. $A = 9448.1$, $B = 0.903$.

12. Pb.

Similar to bismuth, thin superconducting films of lead were studied by Goldman and co-authors [12], which was a continuation of the work of Strongin *et al.* two decades earlier [6]. Both studies involved cold deposition of Pb films. Strongin *et al.* reported some complete datasets for thin Pb films grown on previously deposited SiO_2 , while Goldman and co-authors characterized lead films grown on previously deposited Ge films. Here we present all of these datasets.

12.1. Pb- extracted from Strongin *et al.* [6] ($\blacktriangle, \blacktriangledown, \oplus, \bullet, \bullet$ and \circ in Fig. 4).

As a part of their study of superconductivity in thin films, Strongin *et al.* reported some 7 complete experiments (datasets) of Pb grown on pre-deposited SiO₂ substrates. Six of these datasets were found to fit Eq. 1 very well, while the additional dataset was found to agree with the scaling of dT_c vs. R_s , but the quantitative fitting was less successful (an additional dataset, from which we were able to extract only one data point, was also reported). We present all of these datasets here with the same symbols as in both Fig. 4 and the original paper.

Table S12.1. Superconductivity in Pb (Strongin *et al.* [6]) ▼, ▲, ◊, ●, • and ○ in Fig. 4. d , T_c , and R_s of different sets of Pb films extracted from Strongin *et al.* [6] (Figures 5 and 6 therein). The error in data extraction is evaluated through the error in the extracted T_c values. Values calculated for A , B , T_{c_RC} , and Error in $T_{c_RC}\%$ are also presented. The symbols representing each dataset in both the original paper [6] and in Fig. 4 are also presented.

Symbol:	From Fig. 5		From Fig. 6		Err $T_c\%$	T_{c_RC} [K]	Err $T_{c_RC}\%$		
	R_s [Ω/\square]	T_c [K]	d [nm]	T_c [K]				A	B
▼	88.959	6.753	90.1	6.646	-1.58	7.27	7.67	A	25803
▼	227.956	6.203	51.75	6.197	-0.09	5.83	-6.01	B	0.82
▼	649.151	5.195	25.77	5.4	3.94	4.94	-4.87		
▼	3407.124	2.879	10.74	2.872	-0.23	3.02	5.04		
▲	179.160	6.08							
▲	246.512	5.905	75.99	5.889	-0.26	6.22	5.4	A	14299
▲	400.285	5.44	63.91	5.431	-0.17	5.48	0.75	B	0.619
▲	646.182	4.998	54.38	4.978	-0.4	4.79	-4.17		
▲	978.841	4.39	47.8	4.379	-0.24	4.21	-4.01		
▲	1406.723	4.047	41.61	4.092	1.12	3.87	-4.45		
▲	1935.924	3.546	37.43	3.525	-0.59	3.53	-0.51		
▲	2615.306	3.034	33.25	3.043	0.29	3.3	8.64		
◊	58.064	6.97							
◊	129.108	6.378	68.65	6.362	-0.26	6.53	2.32	A	45805
◊	198.665	6.124	49.78	6.145	0.34	5.97	-2.5	B	0.952
◊	283.058	5.978	37.12	5.907	-1.19	5.72	-4.37		
◊	373.846	5.517	28.31	5.504	-0.23	5.75	4.25		
◊	544.687	5.092	22.43	5.091	-0.01	5.07	-0.39		
●	233.689	5.648	38.08	5.626	-0.39	5.29	-6.28	A	31806

●	327.309	5.335	28.15	5.359	0.45	5.24	-1.83	B	0.928
●	524.138	4.671	18.46	4.671	0	5.16	10.5		
●	873.743	4.058	14.21	4.03	-0.69	4.17	2.84		
●	2214.532	2.667	9.895	2.636	-1.15	2.53	-5.24		
•	29.428	7.128							
•	88.727	6.669							
•	174.642	6.198	69.67	6.196	-0.04	6.13	-1.14	A	47822
•	282.628	5.823	46.94	5.83	0.12	5.86	0.58	B	0.914
•	448.432	5.329	32.9	5.321	-0.16	5.48	2.83		
•	884.198	4.334	23.45	4.32	-0.32	4.13	-4.62		
•	1726.928	3.316	15.6	3.313	-0.07	3.37	1.64		
○	5.193	7.126							
○	31.291	6.926							
○	108.621	6.854	100.7	6.847	-0.1	6.22	-9.25	A	109742
○	203.292	6.045	47.61	6.046	0.01	6.59	9.08	B	1.102
○	308.576	5.569	33.04	5.867	5.35	6	7.73		
○	524.479	4.794	23.55	4.78	-0.3	4.69	-2.17		
○	931.595	3.951	15.59	3.932	-0.48	3.76	-4.8		
▽	840.466	4.289							
▽	1646.527	3.154							
▽	1844.345	2.847							
▽	1927.64	2.304	11.1	2.322	0.76	4.68	103.2		
▽	2662.622	2.623							
▽	2761.538	2.472							
▽	3861.984	1.78							
△	35.891	6.837	210.3	6.835	-0.03	6.58	-3.73		
△	88.045	6.423	173.6	6.44	0.26	3.81	-40.75		
△	138.09	6.122	148.9	6.104	-0.29	3.06	-49.98		
△	202.856	5.888	116.3	5.885	-0.04	2.86	-51.48		
△	317.741	5.379	95.04	5.398	0.36	2.41	-55.11		
△	421.107	5.085	79	5.086	0.01	2.3	-54.71		
△	524.302	4.73	70.03	4.75	0.42	2.17	-54.15		
△	577.377	4.648	59.04	4.632	-0.34	2.38	-48.88		
△	950.854	3.907	50.19	3.93	0.58	1.85	-52.57		
△	1030.484	3.791	39.85	3.791	0	2.18	-42.39		
△	1129.304	3.605	32.61	3.599	-0.16	2.48	-31.35		
△	1296.145	3.486	28.81	3.476	-0.28	2.5	-28.27		
△	1489.056	3.157	25.48	3.153	-0.13	2.52	-20.1		
△	1629.329	3.067	22.46	3.05	-0.56	2.66	-13.4		
△	1781.429	2.874	20.99	2.854	-0.69	2.64	-8.12		
△	1933.836	2.792	18.97	2.791	-0.04	2.73	-2.2		

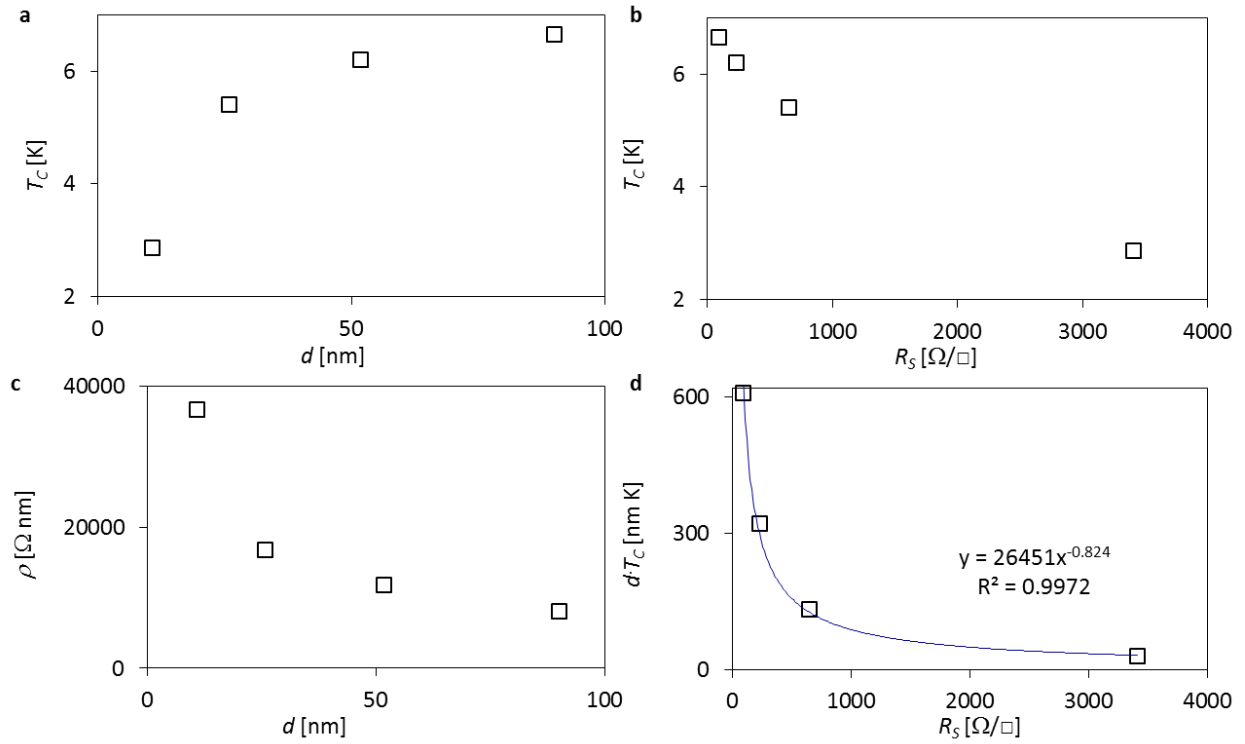


Fig. S12.1. Superconductivity in Pb (Strongin *et al.* [6]), ▼ in Fig. 4. Critical temperature as a function of (a) thickness and (b) sheet resistance. (c) Resistivity as a function of thickness. (d) dT_c vs. R_s . Taken from ▼ in Figures 5 and 6 by Strongin *et al.* [6] $A = 26451$, $B = 0.824$.

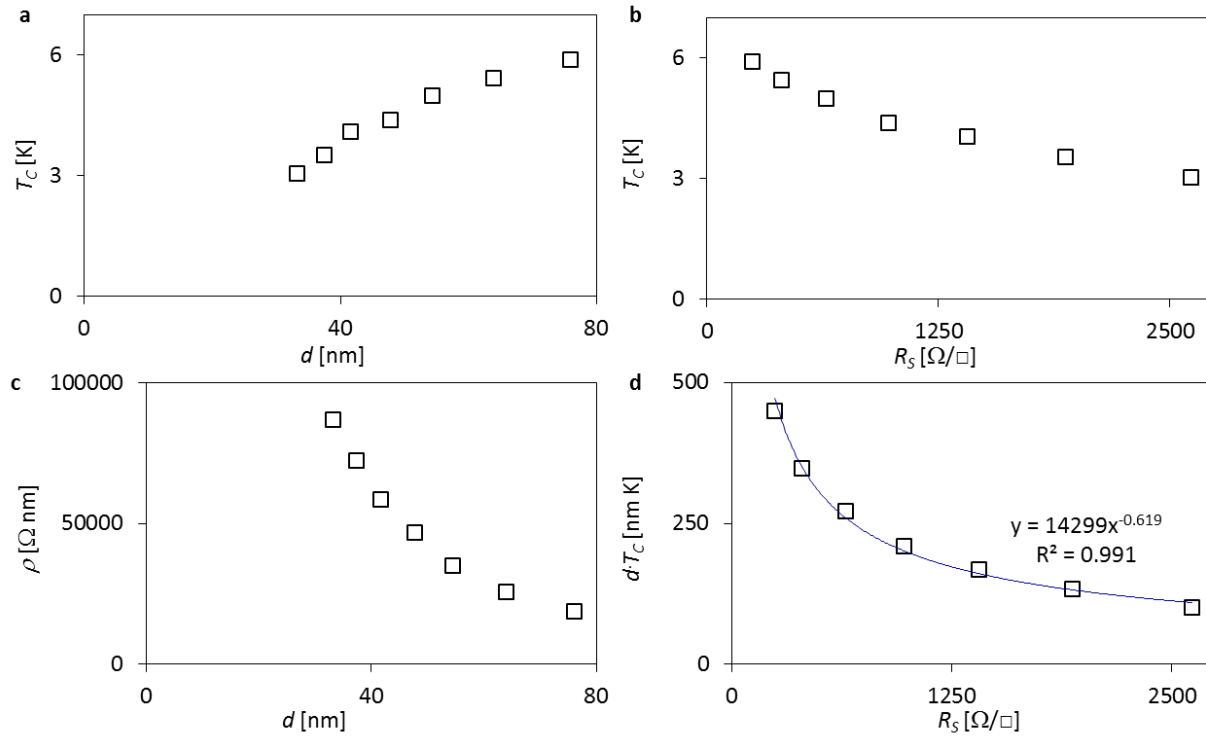


Fig. S12.2. Superconductivity in Pb (Strongin *et al.* [6]), ▲ in Fig. 4. Critical temperature as a function of (a) thickness and (b) sheet resistance. (c) Resistivity as a function of thickness. (d) dT_c vs. R_s . Taken from ▲ in Figures 5 and 6 by Strongin *et al.* [6] $A = 14299$, $B = 0.619$.

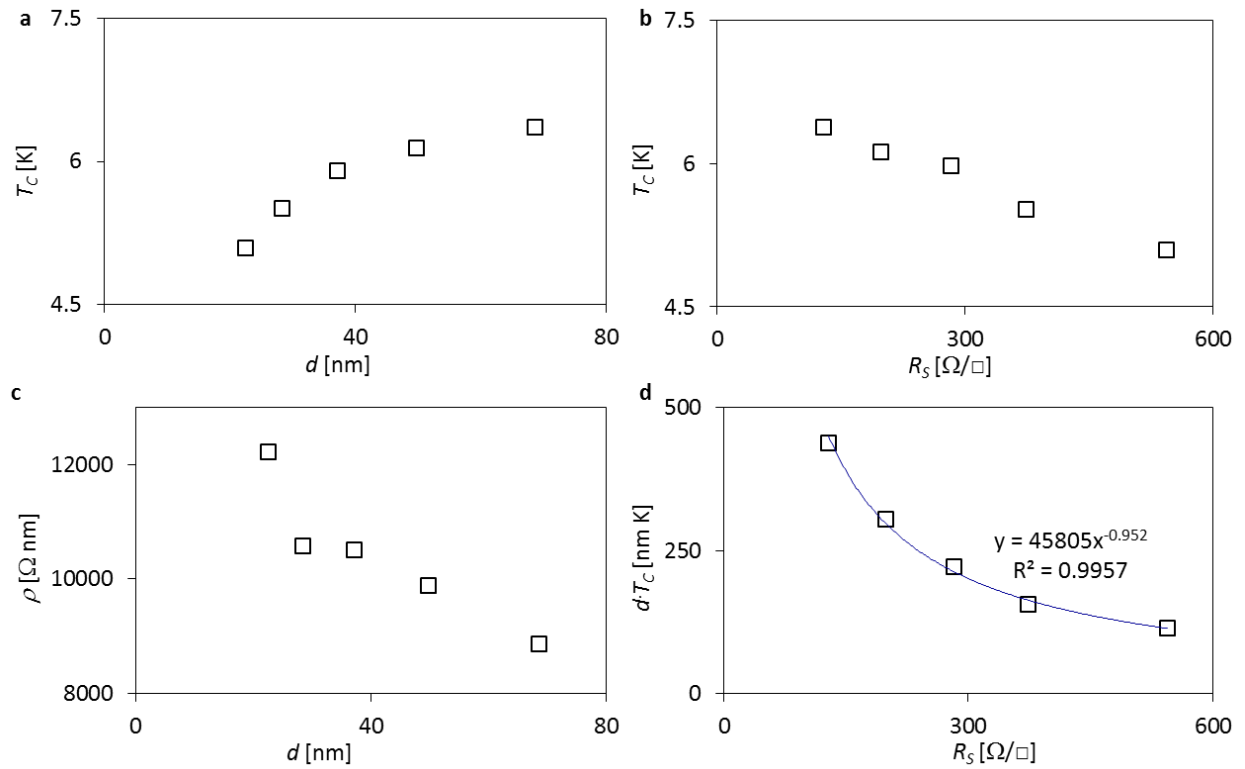


Fig. S12.3. Superconductivity in Pb (Strongin *et al.* [6]), Φ in Fig. 4. Critical temperature as a function of (a) thickness and (b) sheet resistance. (c) Resistivity as a function of thickness. (d) dT_C vs. R_S . Taken from Φ in Figures 5 and 6 by Strongin *et al.* [6] $A = 45805$, $B = 0.952$.

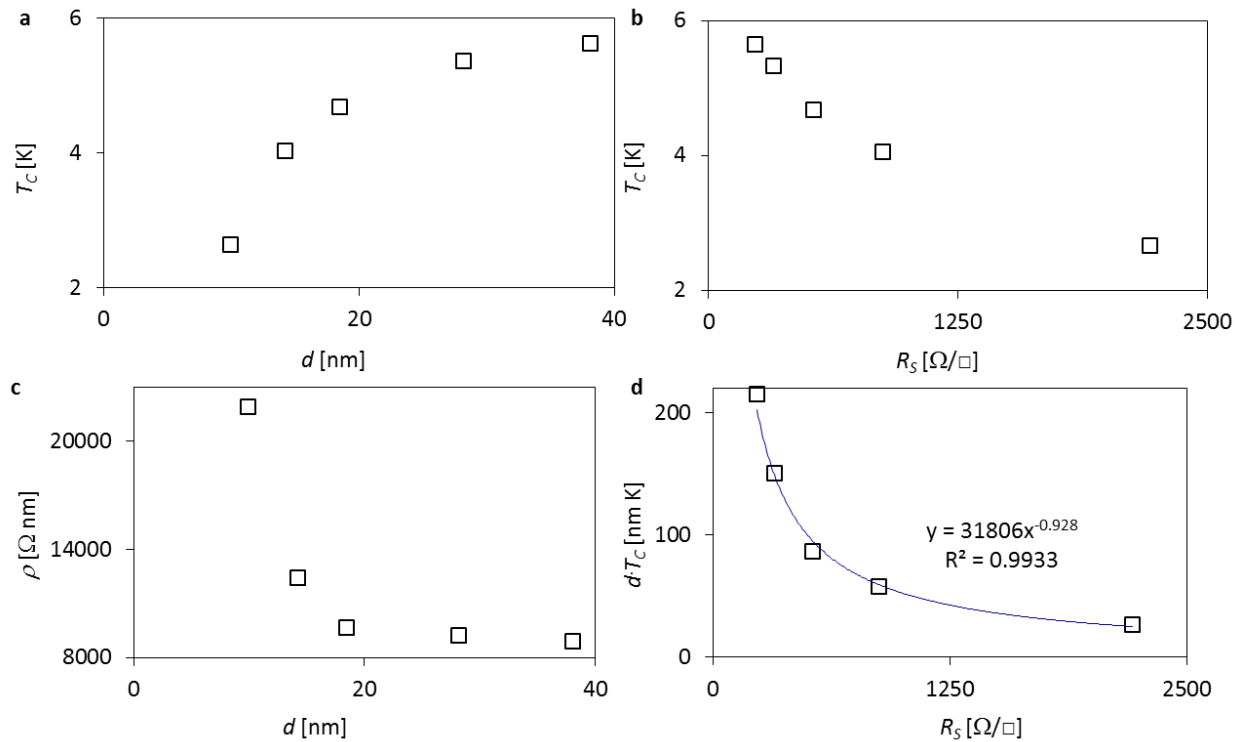


Fig. S12.4. Superconductivity in Pb (Strongin *et al.* [6]), ● in Fig. 4. Critical temperature as a function of (a) thickness and (b) sheet resistance. (c) Resistivity as a function of thickness. (d) dT_c vs. R_s . Taken from ● in Figures 5 and 6 by Strongin *et al.* [6] $A = 31806$, $B = 0.928$.

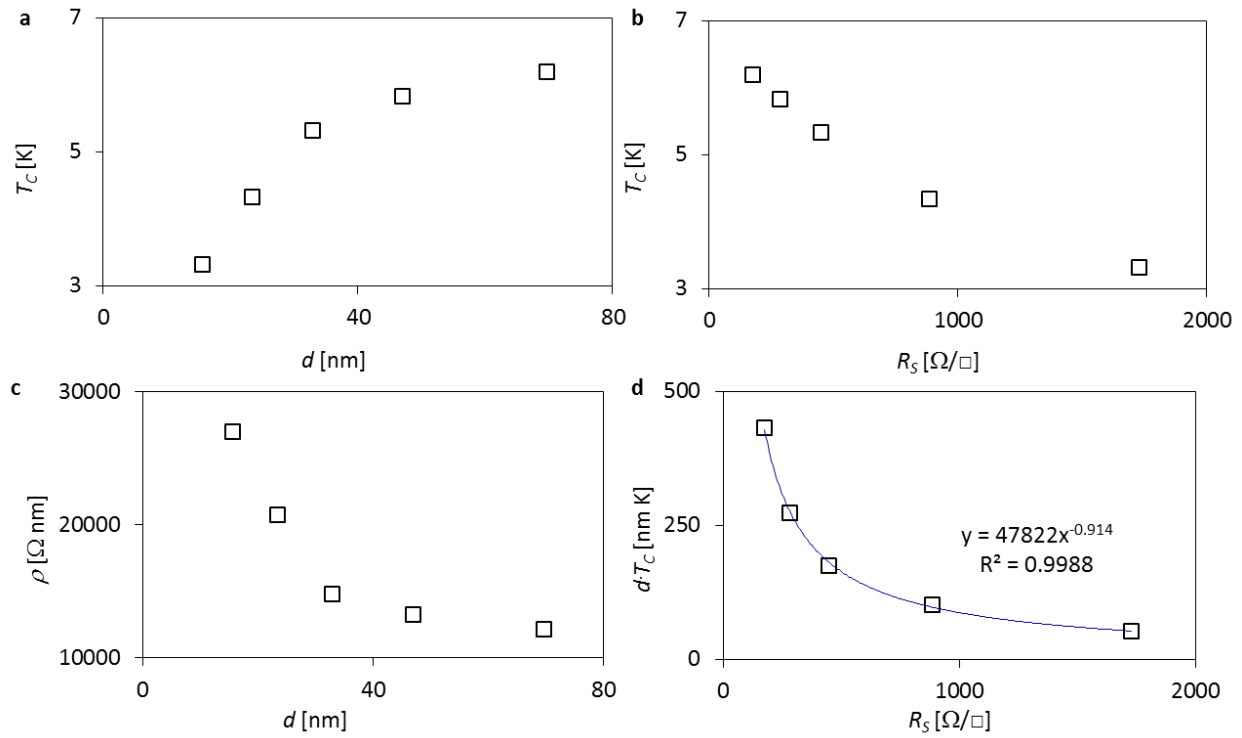


Fig. S12.5. Superconductivity in Pb (Strongin *et al.* [6]), • in Fig. 4. Critical temperature as a function of (a) thickness and (b) sheet resistance. (c) Resistivity as a function of thickness. (d) dT_c vs. R_s . Taken from • in Figures 5 and 6 by Strongin *et al.* [6] $A = 47822$, $B = 0.914$.

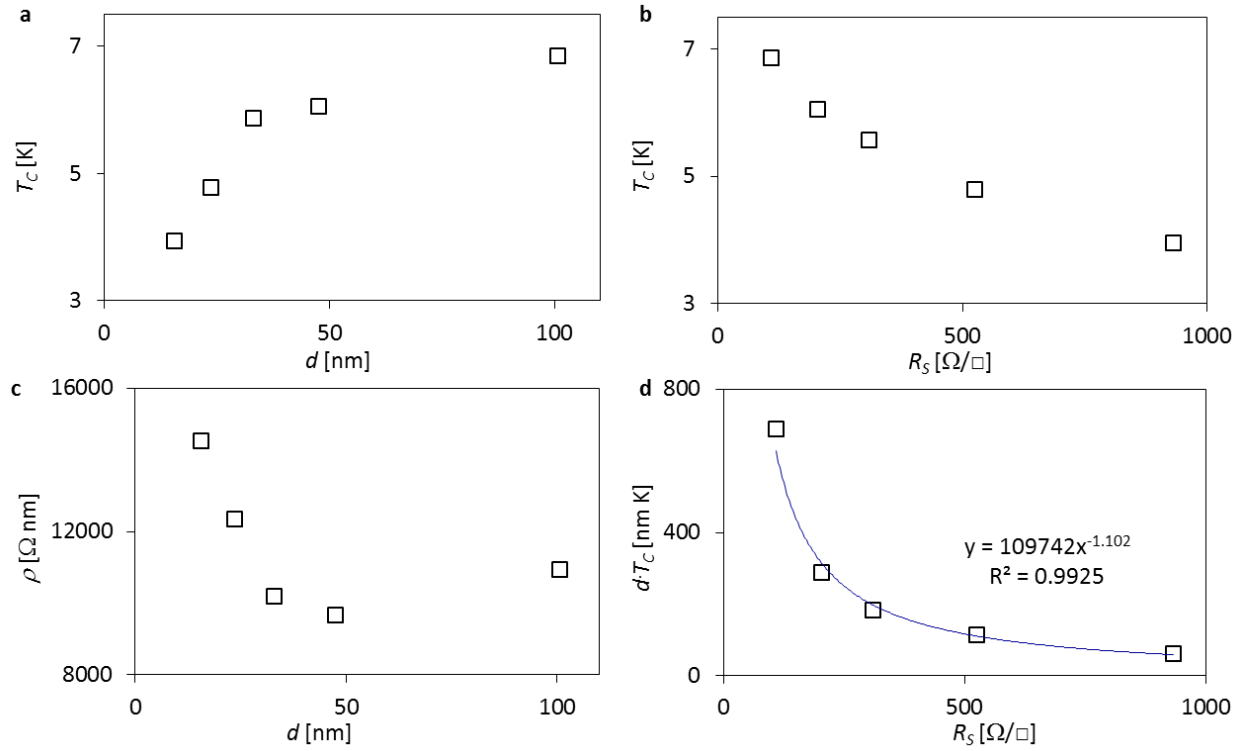


Fig. S12.6. Superconductivity in Pb (Strongin *et al.* [6]), \bigcirc in Fig. 4. Critical temperature as a function of (a) thickness and (b) sheet resistance. (c) Resistivity as a function of thickness. (d) dT_c vs. R_s . Taken from \bigcirc in Figures 5 and 6 by Strongin *et al.* [6] $A = 109742$, $B = 1.102$.

12.7. Pb- extracted from Haviland *et al.* [12] (\triangleleft in Fig. 4).

When Haviland *et al.* studied the quantum transition between superconducting and insulating states (*i.e.*, the ‘onset of superconductivity’), they studied superconductivity in thin Pb films in addition to the classic example of Bi films. They found that Pb films exhibit superconductivity for all films thicker than ~ 0.3 nm. However, since Pb has a typical lattice constant of ~ 0.49 nm [33], we think one can assume that superconductivity at $d < \sim 0.49$ nm cannot be considered as 2D superconductivity of a continuous film. Rather, it is reasonable to assume that films reported to be thinner than 0.49 nm are not homogeneous (or continuous). Hence, we do not expect the mechanism governing superconductivity in these films to be similar to that governing

superconductivity in 2D films. Indeed, a log-log scale plot of dT_c vs. R_s demonstrates linearity of the data for $d > \sim 0.4$ nm. Hence, although we present all the data points below to allow the reader to look at the data more carefully, in Fig. 4 we included only the films thicker than 0.4 nm. Moreover, for the quantitative analysis (extracting A and B), we used only films with $d \geq 0.49$ nm. For the fitting to Eq. 1 we also excluded several films that had relatively high inconsistency in their values as extracted by us (highlighted in red below). It should be noted that in the thinnest films, superconductivity may have been influenced by the proximization with the Ge substrate, hence changing the trend from a power law to a more complex form. An insightful discussion about superconductivity in these Pb films is presented in Section 17.2.

Table S12.2. Superconductivity in Pb (Haviland *et al.* [12]), \triangleleft in Fig. 4. d , T_c , and R_s of Pb films extracted from Haviland *et al.* [6] (Figures 2 and 3 therein). The error in data extraction is evaluated through the error in extracted T_c values. Values calculated for A , B , T_{c_RC} , and Error in $T_{c_RC}\%$ are also presented. Errors in the data extraction larger than 1% are highlighted in red, while films thinner than the nominal lattice constant of Pb are highlighted in blue.

From Fig. 2		From Fig. 4			A	1090.9
d [nm]	T_c [K]	R_s [Ω/\square]	T_c [K]	Err $T_c\%$	B	0.821
					T_{c_RC} [K]	Err $T_{c_RC}\%$
2.89	6.641					
2.725	6.612	57.476	6.546	1.02		
2.551	6.551	68.253	6.452	1.52		
2.364	6.46	53.884	6.641	-2.71		
2.212	6.299	57.476	6.609	-4.69		
2.0877	6.095	107.768	6.294	-3.17		
1.9417	6.005	165.245	6.096	-1.5		
1.795	5.72	280.198	5.72	0.01	5.95	3.96
1.661	5.612	334.082	5.614	-0.04	5.56	-0.87
1.506	5.482	395.15	5.482	0	5.35	-2.48
1.376	5.357	438.258	5.36	-0.06	5.38	0.35
1.239	5.2	510.103	5.207	-0.12	5.27	1.3
1.115	5.068	603.503	5.067	0.03	5.1	0.64

1.001	4.854	725.64	4.847	0.13	4.88	0.61
0.903	4.668	872.923	4.66	0.18	4.65	-0.4
0.855	4.535	951.953	4.53	0.12	4.58	0.9
0.812	4.4293	1070.498	4.419	0.23	4.38	-1.2
0.769	4.2729	1171.082	4.266	0.17	4.29	0.47
0.747	4.2119	1268.074	4.213	-0.03	4.14	-1.73
0.712	4.0501	1386.619	4.049	0.02	4.04	-0.36
0.683	3.9653	1508.756	3.97	-0.12	3.92	-1.05
0.662	3.8486	1623.709	3.838	0.28	3.81	-0.94
0.639	3.7559	1774.585	3.759	-0.07	3.67	-2.32
0.613	3.6179	1914.683	3.621	-0.1	3.59	-0.71
0.570	3.3528	2306.242	3.355	-0.06	3.32	-1.1
0.545	3.1937	2539.74	3.194	-0.01	3.21	0.41
0.517	3.0241	2830.714	3.02	0.14	3.09	2.3
0.491	2.8226	3197.126	2.819	0.11	2.95	4.35
0.469	2.6052	3635.384	2.601	0.17		
0.445	2.3373	4174.225	2.332	0.24		
0.426	2.1092	4774.136	2.108	0.05		
0.407	1.9024	5309.385	1.965	-0.16		
0.4	1.7884	5560.844	1.787	0.08		
0.392	1.6876	5841.042	1.692	-0.28		
0.386	1.6373	6056.578	1.637	0.01		
0.38	1.4887	6387.068	1.484	0.3		
0.372	1.3827	6555.905	1.382	0.09		
0.36	1.128	7457.566	1.127	0.12		
0.349	0.9663	8007.185	0.961	0.53		
0.34	0.616	9052.537	0.611	0.75		

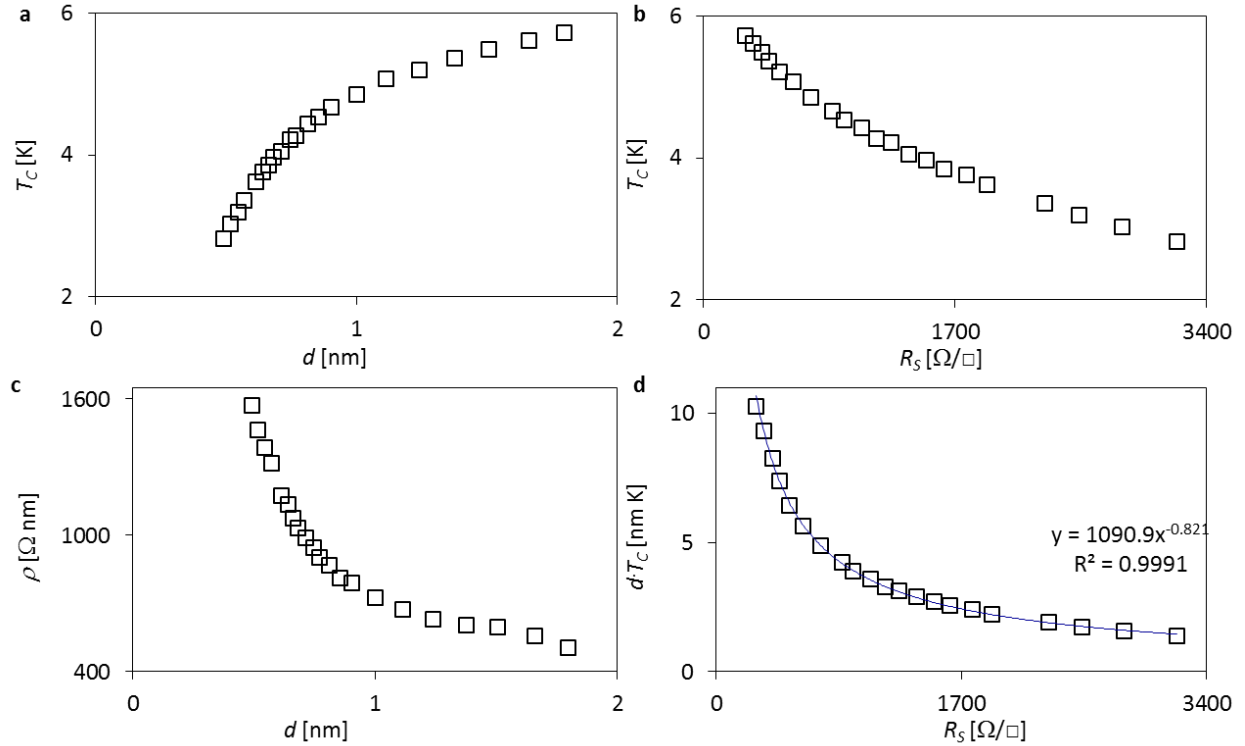


Fig. S12.7. Superconductivity in Pb (Havliand *et al.* [12]) ◀ in Fig. 4. Critical temperature as a function of (a) thickness and (b) sheet resistance. (c) Resistivity as a function of thickness. (d) dT_c vs. R_s . Inconsistent data and films thinner than the nominal lattice constant of Pb are not included (see Table S12.2). $A = 1090.9$, $B = 0.81$.

13. α -ReW- extracted from Raffy *et al.* [34], * in Fig. 4.

Raffy *et al.* reported a set of amorphous ReW films ranging from ~ 4.5 nm to ~ 100 nm thick. The different films varied in stoichiometric composition. Similarly to Graybeal and Beasley [17], they deduced that their data fit the Maekawa and Fukuyama model [35]. In this framework, the electrons are localized, resulting in enhanced electron-electron Coulomb interaction, which in turn suppresses T_c . Practically, from the perspective of the current report, this means that T_c is a function of the sheet resistance only ($T_c = T_c(R_s)$), similar to Finkel'stein's model [22], which is the successor of Maekawa and Fukuyama's model. Raffy *et al.* reported that they believe the properties

of their films do not vary by much, despite their different stoichiometric compositions. However, for each stoichiometry, there were not more than ~3 films to allow a more complete examination of this claim with respect to the scaling we propose here. Moreover, the thickness of the grown films was not equally distributed among the collected data points, a fact that does not allow conclusive quantitative examination of the empirical law of Eq. 1. Yet, we also present the quantitative fitting parameters of this data set to Eq. 1. Furthermore, we present this fitting on a log-log scale similar to that of Fig. 4 in the main text. In this respect, it is interesting to note that the parameters for A and B are in agreement with the linearity in Fig. 5a.

We should mention here that one of the data points was found to behave differently than its sisters. This was noticeable for instance in its resistivity, which is more than 50% higher than the average resistivity of the other films. Hence, although this film is presented below, we did not include it for the quantitative fit.

Table S13. Superconductivity in α -ReW (Raffy *et al.* [34]), * in Fig. 4. d , T_c , R_s , and the composition of α -ReW films extracted from Raffy *et al.* [34] (Fig. 1 therein). The error in data extraction is evaluated through the error in extracted T_C values, which are also presented. Values calculated for A , B , T_{c_RC} , and Error $T_{c_RC}\%$ are also presented. Films that not all of their properties are known (T_c , d , and R_s) are highlighted in red. A film that seemed to be different than its sister films is highlighted in blue and was not used for the quantitative fitting.

Composition	From Fig. 1 Top		From Fig. 1 Bottom			A	14545
	d [nm]	T_c [K]	R_s [Ω/\square]	T_c [K]	Err T_c %	B	1.078
Re70W30	106.8296	6.811	14.828	6.732	-1.15	T_{c_RC} [K]	7.44
Re70W30	10.26937	5.3	158.483	5.3	-0.02	$T_{c_RC}\%$	9.24
Re70W30	5.051	4.047	421.556	4.031	-0.39		6.02
Re 65W35	9.709	5.242	187.98	5.292	0.96		4.26
							5.36
							1.07

Re 65W35	5.051	4.371	465.7	4.327	-1.02	3.83	-12.39
Re60W40	11.691	5.343	141.357	5.383	0.76	5.98	11.96
Re60W40	5.051	3.771	385.566	3.789	0.46	4.69	24.47
Re55W45	106.974	6.368	18.7	6.256	-1.75	5.79	-9.14
Re55W45	15.392	5.587	128.179	5.588	0.03	5.05	-9.63
Re55W45	7.092	4.77	277.806	4.722	-1.01	4.76	-0.22
x Re50W50	9.174	4.619	239.005	4.601	-0.38	4.33	-6.31
X Re50W50	4.525	3.487	545.099	3.499	0.34	3.61	3.44
▽ Re50W50	10.142	4.7	257.292	4.669	-0.66	3.62	-23.08
Re 65W35	107.091	6.03	29.073	6.082			
Re70W30			55.753	6.021			
Re70W30			335.876	4.062			
▽ Re50W50	0.02	3.492					

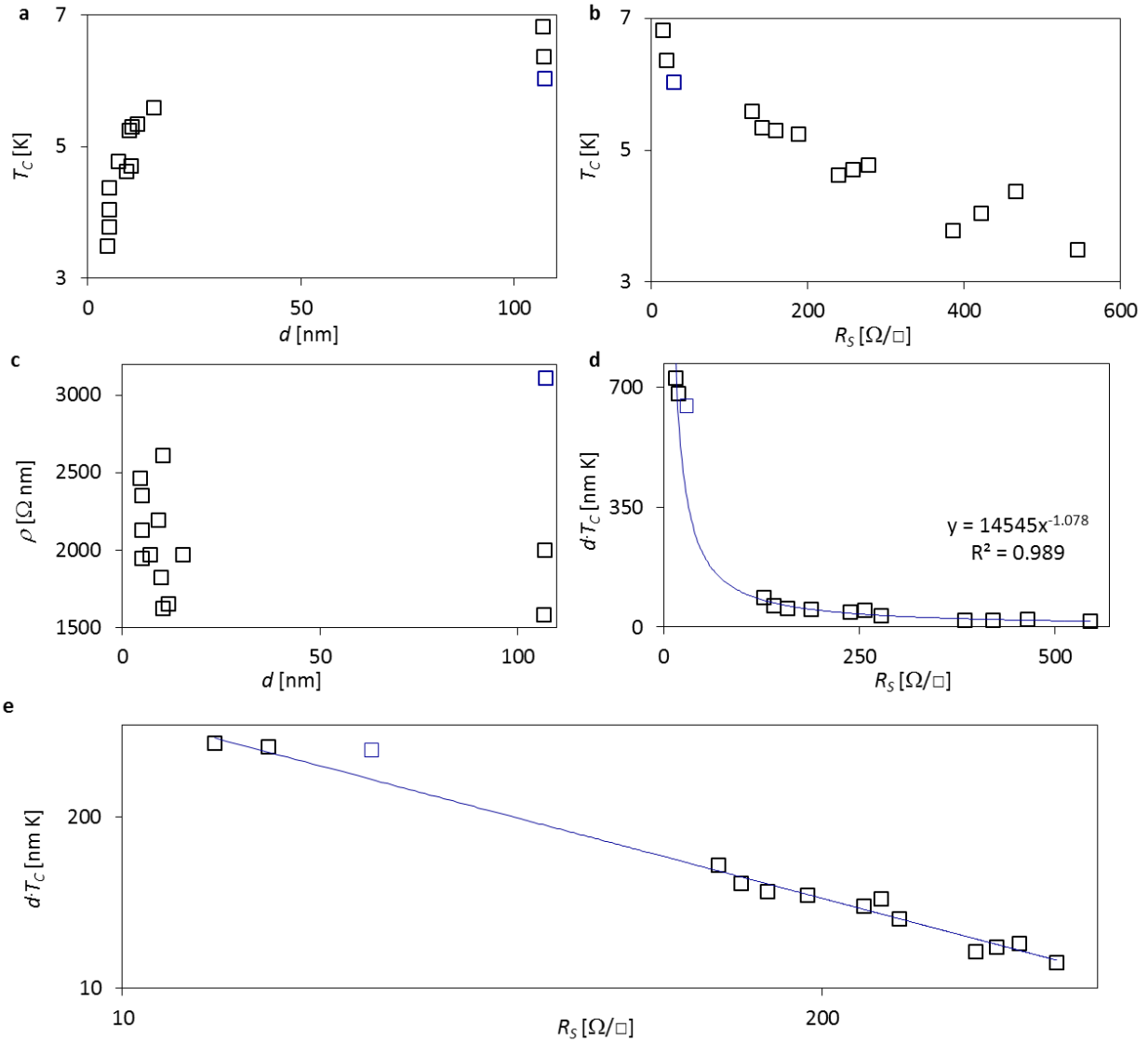


Fig. S13. Superconductivity in α -ReW (Raffy *et al.* [34]), * in Fig. 4. Critical temperature as a function of (a) thickness and (b) sheet resistance. (c) Resistivity as a function of thickness. (d) dT_c vs. R_s on a linear scale with the best fit to Eq. 1 (blue curve). (e) dT_c vs. R_s on a log-log scale with the best fit to Eq. 1 (blue curve). The point appears in blue in (a-e) was not included in the fitting, as mentioned above. $A = 14545$, $B = 1.078$.

14.4. Sn- extracted from Strongin *et al.* [6].

In addition to the Al and Pb set of films that are discussed above, Strongin *et al.* reported thin superconducting films of Sn [6]. Specifically, they observed an increase in T_c when films get thinner. This T_c increase is followed by suppression of superconductivity for films thinner than ~27 nm. Unlike the cases of Al and the various data sets for Pb, the Sn films seem not to agree well with the scaling of Eq. 1. Here we present these data. We should mention that Goldman and co-authors also studied Sn films [14]. However, we could not find the R_s values of these films, which prevented us from examining their agreement with Eq. 1. One possible explanation for this deviation is the role of proximity effect as discussed in Section 17.2.

Table S14. Superconductivity in Sn films (Strongin *et al.* [6]). d , T_c , R_s , and the composition of Sn films extracted from Strongin *et al.* [6] (Fig. 2 therein). The error in data extraction is evaluated through the error in the extracted d values, which are also presented. Films for which we could not find the complete data are highlighted in red.

From Fig. 2 Top		From Fig. 2 Bottom		
d [nm]	T_c [K]	d [nm]	R_s [Ω/\square]	$Err\ d\%$
16.215	4.2833	16.128	778.531	-0.54
19.202	4.8223	19.538	555.91	1.75
22.577	5.2652	22.489	469.144	-0.39
27.621	5.885	27.477	309.42	-0.52
33.494	4.6815	33.171	194.123	-0.96
38.475	4.5528	9.9705	8773.079	

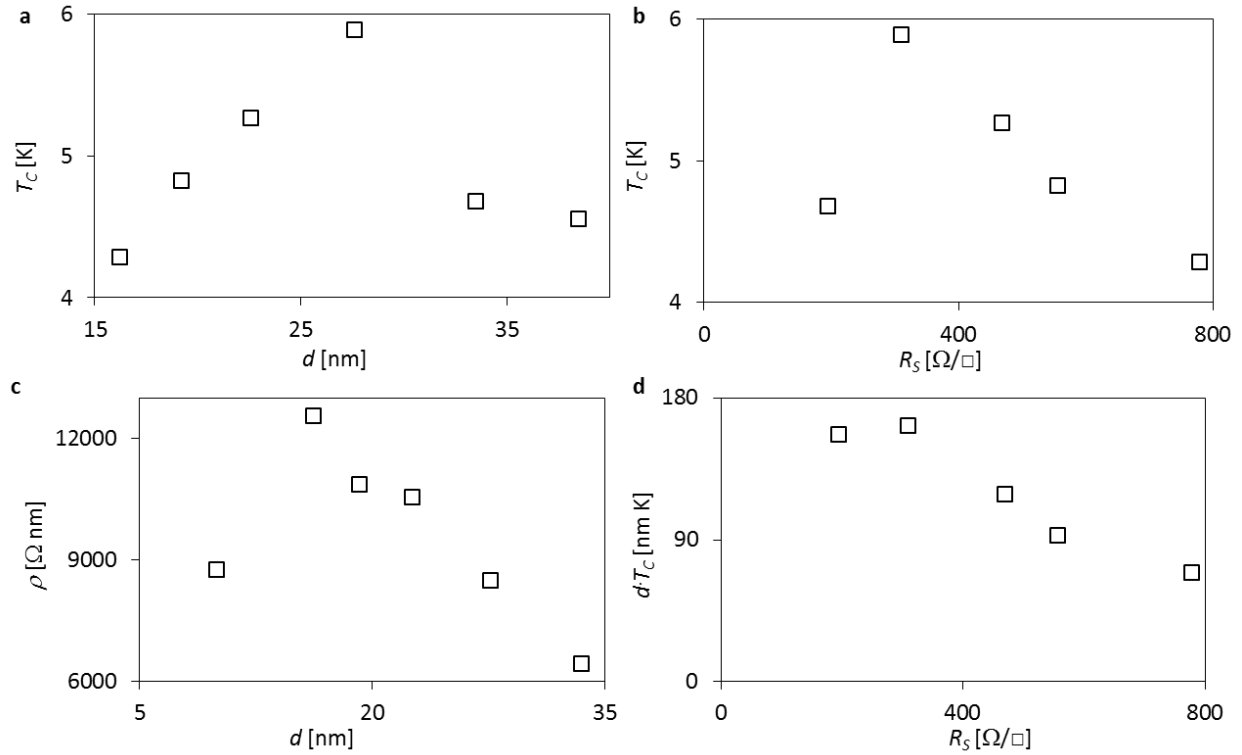


Fig. S14. Superconductivity in Sn films (Strongin *et al.* [6]). Critical temperature as a function of (a) thickness and (b) sheet resistance. (c) Resistivity as a function of thickness. (d) dT_c vs. R_s .

15. TiN

Thin TiN films are considered highly disordered superconductors. In fact, it is believed that they can undergo a superconducting-to-superinsulating transition [36]. Being ‘exotic’ disordered superconductors, it is interesting to realize that TiN films grown by different groups agree with the found scaling. In particular, we demonstrated that the discovered scaling describes well the properties of films reported by Klapwijk and co-authors [37,38] and those reported by Baturina and co-authors [39].

Typically, TiN films are grown with the atomic layer deposition method (ALD). In this method, a precursor material is used. For the discussed TiN films, this material is Cl. Due to their chemical

properties, the Cl atoms interact with the films and usually some Cl atoms remain in the film and cannot be removed. These Cl atoms give rise to Columbic and magnetic impurities in the system, which in turn affect the inhomogeneity of the films and influence the inherent disorder. The influence of the Cl atoms on the metallic and superconducting properties of the films are not fully known, and it is also not known whether these effects are thickness dependent. Sometimes, the Cl concentration can be measured, but even when it is the case, this concentration cannot be reduced or controlled de-facto significantly. Moreover, it is unknown whether the Cl atoms are distributed in the films homogeneously or not. Yet, the data analyzed below demonstrate that despite the potential effects of the Cl atoms, the sets of films grown under similar conditions follow the discovered scaling $dT_c(R_s)$

15.1. TiN- extracted from (Klapwijk and co-authors [37,38]), ☆ in Fig. 4.

Thin TiN films are considered as highly-disordered superconductors. As such, Driessen *et al.* reported a set of TiN films grown on SiO substrates, suggesting that their superconducting properties do not comply with the conventional theory [37]. This was followed by a growth of a set of thinner films reported by Coumou *et al.* [38]. In fact, Klapwijk and co-authors *et al.* suggested that the electric properties of these films in the normal state also deviate from conventional theory (*ibid*). Although the authors suggested a heuristic electrodynamic analysis, they claim that their observations are not yet understood and have to be clarified. Hence, we examined the properties of these highly resistive films ($\rho = 120\text{-}380 \mu\Omega \text{ cm}$) with Eq. 1. Surprisingly, we found that, similar to the other materials examined above, these highly disordered TiN films fit Eq. 1 with a very good agreement. Moreover, by merging the two sets of films we can suggest that they may not be very different with respect to their superconducting and metallic properties. We should note that we believe that one of these films is different in nature than the

others. Alternatively, the reported thickness of this film might be thinner than the actual value. This can be determined from, *e.g.*, the dependence of resistivity on thickness, as presented in Fig. S15c, which suggests that its thickness is ~ 9.5 nm instead of the nominal 6 nm. Alternatively, a value of T_c higher than the one reported in the paper can also explain the deviation. Hence, for the quantitative analysis, we did not include this film. However, we do present its values quantitatively and graphically in Table S15 (designated in blue) and Fig. S15d (designated in red). Moreover, we can also mention that, given $d = \sim 9.5$ nm, as suggested by the $\rho(d)$ curve, this film also agrees with the other data for the dT_c vs. R_s curve (Fig. S14d). We would like to update the reader that prior to publication, after having corresponding with Klapwijk and co-authors, we were informed that indeed, the film that we predicted to have values different than those reported in the literature were re-measured, and indeed, the value of T_c was found to be higher than the value reported in Ref. [37]. Hence, this prediction signifies the usefulness of the model that can be used also to predict the superconducting behavior of thin films.

Lastly, we should mention that Driessen *et al.* also reported highly disordered NbTiN films as well as TiN on a different substrate. However, these sets included too few films to allow an examination of Eq. 1.

Table S15.1. Superconductivity in highly-disordered TiN films (Klapeijk and co-authors [37,38]), ☆ in Fig. 4. d , T_c , and R_s of disordered TiN films extracted from Klapeijk and co-authors [37,38] (Table 1 in Ref. [37] and Supplemental Material in [38]). A film with a nominal thickness smaller than that we believed is highlighted in blue.

All from [37,38] but red point		From [37] without blue point		From [37]		All from [37,38]	
A	2784.7	A	2825.6	A	3889.6	A	2678.6
B	0.811	B	0.817	B	0.906	B	0.812

d [nm]	T_C [K]	R_S [Ω/\square]	T_{C_RC} [K]	Err $T_{C_RC}\%$	T_{C_RC} [K]	Err $T_{C_RC}\%$	T_{C_RC} [K]	Err $T_{C_RC}\%$	T_{C_RC} [K]	Err $T_{C_RC}\%$
89	3.6	13.48315	3.79	5.12	3.79	5.4	4.14	14.98	3.64	1.12
45	3.2	41.55556	3.01	-6.24	2.99	-5.87	2.95	-7.73	2.89	-9.8
22	2.7	115	2.7	-0.05	2.66	-0.05	2.4	-11.05	2.58	-4.32
11	2.2	323.6364	2.33	5.66	2.29	6	1.88	-14.5	2.23	1.37
6	1.5	633.3333	2.48	39.52	2.42	65.35	1.88	25.14	2.37	58.03

All from [37,38] but red point

From [38]

All from [37,38]

d [nm]	T_C [K]	R_S [Ω/\square]	A		B		A		B	
			T_{C_RC} [K]	Err $T_{C_RC}\%$	T_{C_RC} [K]	Err $T_{C_RC}\%$	T_{C_RC} [K]	Err $T_{C_RC}\%$	T_{C_RC} [K]	Err $T_{C_RC}\%$
			2784.7		8787		2678.6		0.812	
			0.811		0.957					
4	0.7	4300	0.79	11.05	0.73	4.58	0.75	7.24		
4.3	0.78	3700	0.83	5.68	0.79	0.81	0.79	1.15		
4.5	0.99	3000	0.94	-5.69	0.92	-7.23	0.89	-9.71		
4.8	1.3	2000	1.22	-6.55	1.27	-2.37	1.16	-10.4		
5	1.5	1500	1.48	-1.41	1.6	6.97	1.41	-5.84		
5.5	1.6	1400	1.42	-12.52	1.56	-2.61	1.36	-15.13		

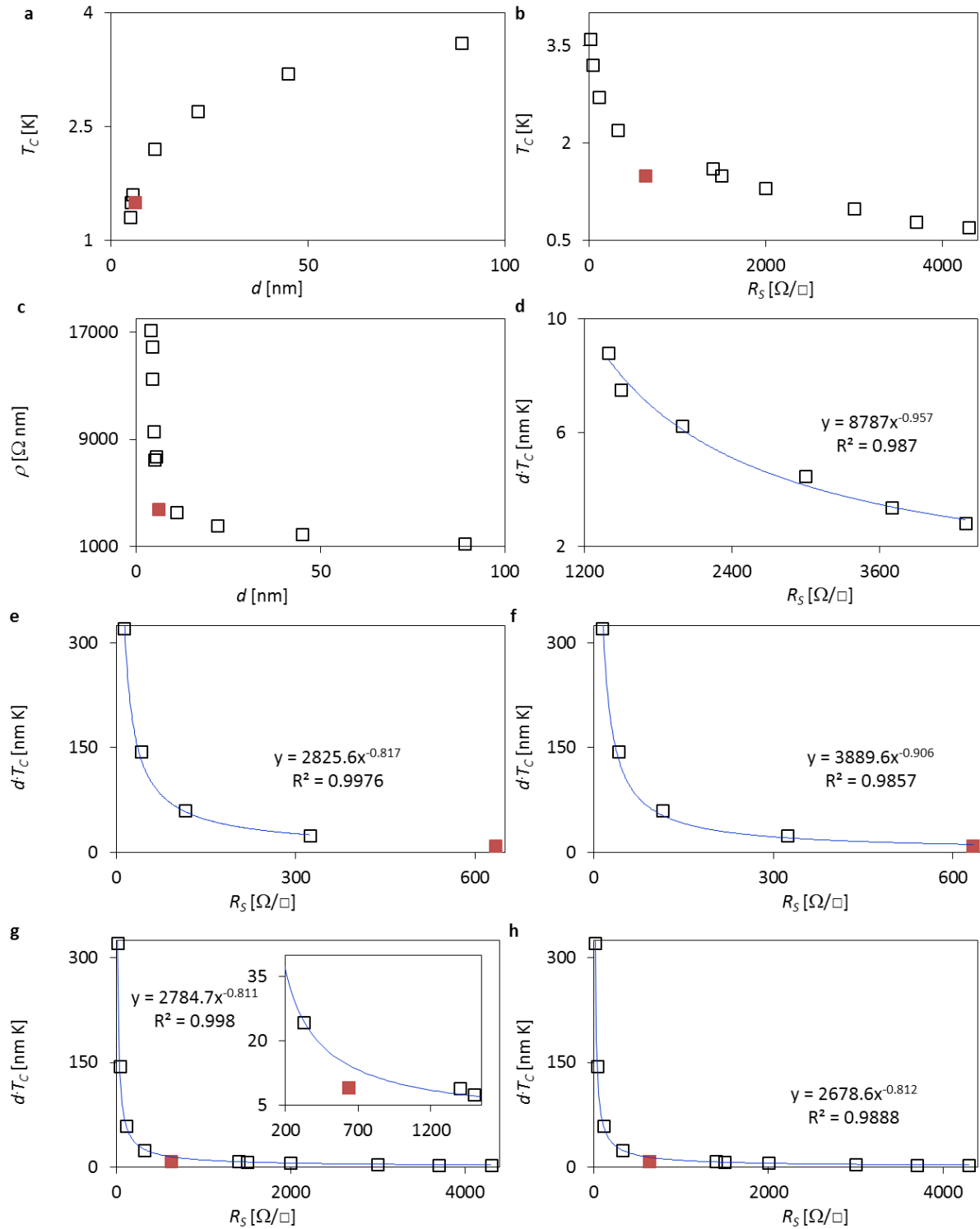


Fig. S15.1 Superconductivity in in highly-disordered TiN films (Klapwijk and co-authors [37,38]), ☆ in Fig. 4. Critical temperature as a function of (a) thickness and (b) sheet

resistance. (c) Resistivity as a function of thickness. (d) dT_c vs. R_s with the best fit of the films from Ref. [38] for Eq. 1. (e) Fitting the data from Ref. [37] to Eq. 1 excluding and (f) including the red data point that corresponds to the blue values in Table S14 (as discussed in the text). (g) Fitting all the data from both Ref. [37,38] to Eq. 1, while excluding the red data point. Inset is a closer look at the area around the red point, emphasizing that this film is different than the others. (h) Fitting the entire set of films from Ref. [37,38] to Eq. 1 (including the red data point).

15.2 TiN- extracted from (Baturina and co-authors [37]), ☆ in Fig. 4.

Baturina and co-authors have also reported on TiN films. These films were grown by atomic layer deposition (ALD). Since in this method traces of Cl atoms exist in the sample, variation in Cl concentration can derive changes in the homogeneity, disorder and other superconducting- and metallic –related properties. Baturina and co-authors measured the Cl concentration in their films and were able to form a set of films with a constant value of the Cl concentration. We should note that, even though the concentration is the same for the data set, the Cl might not be homogeneously distributed in the film and the Cl atoms do expect to affect the measured properties of the films in a way that might, or might not, be thickness dependent. To measure the thickness, Baturina and co-authors imaged the films with transmission electron microscopy, allowing a direct measurement of the film thickness.

Similarly to the case of Al and Sn, the films from Baturina and co-authors seem to exhibit a small enhancement in T_c in the thicker film regime. This increase in T_c cannot be explained in the $T_c(R_s)$ or $T_c(d)$ graphs, but is consistent with the other data points in the $dT_c(R_s)$ scale.

We should note that although the data from Baturina and co-authors and the data from Klapijk and co-authors do not coincide in most other scaling, the grown films looks more similar when are compared on a $dT_c(R_s)$ graph.

Table S15.2 Superconductivity in highly-disordered TiN films (Baturina and co-authors [36]),

★ **in Fig. 4.** d , T_c , and R_s of disordered TiN films extracted from Baturina and co-authors [36].

			A	1714.7
			B	0.747
d [nm]	T_c [K]	R_s [Ω/\square]	T_{c_RC} [K]	Err T_{c_RC} %
23	3.14	65	3.3	4.78
18	3.315	90	3.3	-0.32
12	3.25	165	3.15	-3.12
10	3.18	216	3.09	-2.82
7	3	334	3.19	5.97
5	2.538	855	2.21	-14.67
3.6	1.26	2520	1.37	8.1

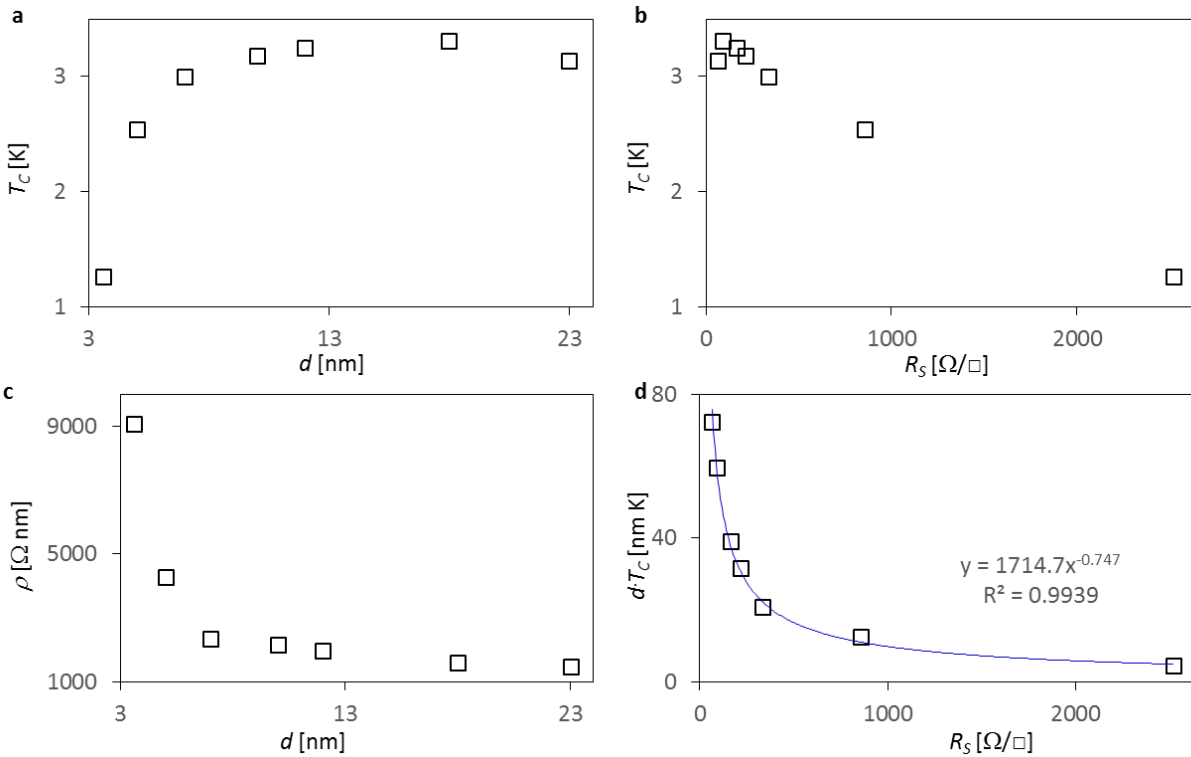


Fig. S16. Superconductivity in highly-disordered TiN films (Baturina and co-authors [37]),

★ in Fig. 4. Critical temperature as a function of (a) thickness and (b) sheet resistance. (c) Resistivity as a function of thickness. (d) dT_c vs. R_s with the best fit for Eq. 1.

16. V₃Si- extracted from Orlando *et al.* [26].

In addition to Nb₃Sn films, Orlando *et al.* also studied superconductivity in highly damaged or highly defected V₃Sn films. The suggestion of the authors that “since the samples were deposited in a ‘compositional phase spread’ configuration, the unpatterned samples vary to some degree in composition across the films” [26] also addresses V₃Sn. In this set of experiments, one film was 1 μm thick, while all the others had $d = 300$ nm (*i.e.*, small thickness distribution with no ‘true’ 2D films), while their R_s , T_c and ρ values varied (the latter had up to 700% difference in range). Therefore, similar to the Nb₃Sn case, this is one of the only examples where our scaling dT_c vs. R_s does not seem to work. Lastly, these films also were examined over the course of two calendar years, which may have allowed their degradation. Hence, the fact that these films do not agree with the proposed scaling does not necessarily invalidate it. We report the data for these films below.

Table S17. Superconductivity in V₃Si (Orlando *et al.* [26]). d , T_c , and R_s of V₃Si films extracted from Orlando *et al.* [26] (Table 1 therein).

T_c [K]	R_s [Ω/□]	d [nm]
16.4	0.052	1000
16.1	0.24	300
15.7	0.503	300

15.6	0.203	300
14.8	1.04	300
14.3	1.263	300
13.9	1.317	300
13.8	1.42	300
13.6	1.44	300
12.9	1.42	300

17. Presentation of all unprocessed data.

Above, we discussed each of the data sets for thin superconducting films individually. In particular, we demonstrated how almost all of these data sets agree with the scaling $dT_c(R_s)$ as well as with the power law of Eq. 1. Moreover, whenever applies, we discussed possible sources of error in the data extracted from the literature as well in the film characterization. Hence, we would like to discuss again the entire data as a whole. Specifically, we would like to elaborate on two issues. First, we would like to elaborate on the fact that based on Fig. 5a, the two fitting parameters (A and B) described in Eq. 1 may be correlated, simplifying the power law. Second, despite the nominated possible sources for errors in the values analyzed in the Supplemental Material, we would like to present the complete, unprocessed data together on one graph. This may supply the reader with the possibility to qualitative estimate the upper limit error of the Eq. 1.

17.1. Possible correlation between A and B .

As mentioned in the main text, the fact that the data presented in Fig. 5a demonstrates a linear trend for more than five orders of magnitude suggests that the parameters A and B (Eq. 1) are correlated. Linearity on such a log-normal scale indicates an exponential relation between A and B . We present again the relation between A and B for the surveyed materials, while we added a linear line (red) to guide the eyes and demonstrate the linearity (Fig. S17.1), suggesting that:

$$\text{Log}(A) = \alpha' + \beta'B \quad (\text{Eq. S1})$$

where α' and β' correspond to the intercept and slope of the red line in Fig. S17.1, respectively.

The exponential dependence of A on B can be substituted in Eq. 1, while it is more appealing to define $\alpha = 10^{\alpha'}$ and $\beta = e^{\beta' \ln(10)}$ and to substitute Eq. S1 in scaling law as appears in Eq. 2a:

$$T_c = \frac{\alpha}{d} \cdot e^{-B \left(\ln \left(\frac{R_s}{\beta} \right) \right)} \quad (\text{Eq. S2a})$$

In this way, the only parameter that represents a certain set of films is the parameter B , while α and β are universal constants. In particular, the parameter β represents a universal constant for a resistance value.

In fact, the red line in Fig. S17.1 used to guide the eye is also the best fit calculated for the possible exponential dependence of A on B , with $\alpha' = 1.14$ and $\beta' = 2.67$ and with the corresponding standard errors of 0.27 and 0.26. That is, Eq. S2a becomes:

$$T_c = \frac{13.7}{d} \cdot e^{-B \left(\ln \left(\frac{R_s}{464} \right) \right)} \quad (\text{Eq. S2b})$$

where we remind the readers that we use T_c , d and R_s in K, nm and Ω/\square .

The value $\beta = 464 \Omega/\square$ is very different from the quantum resistance $\hbar/4e = 6.45 \text{ k}\Omega$. However, this difference is not surprising when bearing in mind that the quantum resistance is not a universal value and that different models use different constants for the sheet resistance [22]. Fig. S17.1 shows that many of the material sets are crowded around $B = 1$. Although the scatter around the Eq. S2b is smaller at the extreme points along the curve, and larger around $B = 1$, it worth mentioning that for the case of B equals to unity, Eq. S2b becomes: $T_c = e^{-\ln(R_s/6355)}/d$, while the 6355 Ω/\square in the exponent is when we used again T_c , d and R_s in K, nm and Ω/\square . We should remind

the reader that an examination of the validity of Eq. S2b and a comparison of the fitting made with this equation to Eq. 1 are discussed in Section 7.1 for the case of α -MoGe.

One may identify that one material is rather far from the linear fit (molybdenum, designated by Δ). Hence, although Fig. S17.1 demonstrates an exponential trend in the dependence of A on B and although the data fit such an exponent quantitatively with a reasonable agreement (Eq. S2b), there is still uncertainty with regard to the limits of the framework of Eq. S2b. Yet, examining the materials at the two extreme points of the linear curve (α MoGe and Al) suggests that the position of the different materials along the curve is determined by its disorder and homogeneity (with respect to stoichiometry, granularity etc). We should note that if we discard the data for Mo, α' and β' almost do not change ($\alpha'_{\text{noMo}} = 1.23$ and $\beta'_{\text{noMo}} = 2.64$), the standard errors are reduced significantly from 0.26 and 0.26 to 0.14 and 0.14, respectively.

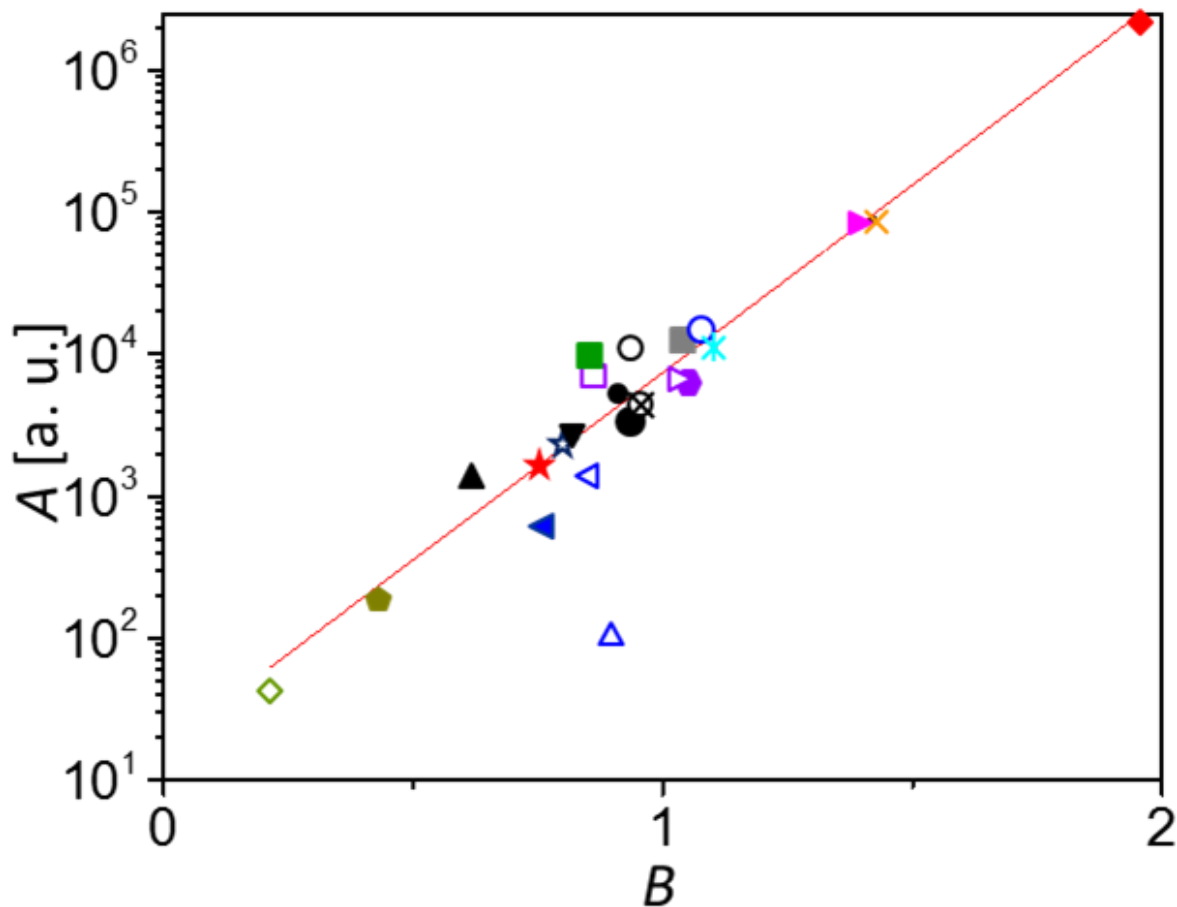


Fig. S17.1. Intercept versus slope (A vs. B) of the best fits for the different data sets to Eq. 1 (reproduced from Fig. 5a). The values for A vs. B for the different sets of materials as were calculated in 1-16 on log-normal axes. The red line is the best fit to Eq. S1, suggests that the parameters A and B are correlated with $\alpha' = 1.14$ and $\beta' = 2.67$ and with the corresponding standard errors of 0.26 and 0.26. The symbols used here are similar to those specified in Fig. 4, including the Mo (designated by \triangle) sample that unlike the other materials, seems to deviate from the linear trend. Without the Mo films, the parameters become: $\alpha'_{\text{noMo}} = 1.23$ and $\beta'_{\text{noMo}} = 2.64$, with the standard error of 0.14 for both.

An additional explanation for the dependence of A on B could be that although the fit to a power law is rather accurate, a different expression is hidden in Eq. 1. In particular, when dealing with universal relations, often, a power law dependence with correlated A and B may imply that Eq. 1 can be rewritten as: $dT_c = A' n / (R_s \ln^n(R_s))$, where A' is a global parameter and $n \ll 1$ is an exponent specific to each material. Such an explanation would be valid only in the limit $B \sim 1$. However, although most of the materials do have indeed an exponent around unity, the scatter of the graph, and hence the deviation from the linear fit in Fig. S17.1 are rather large. Moreover, this cannot explain the materials with $|B-1| \gg 0$. This means that the merit of such logarithmic approximation is low either due to the scatter of the data, where the mathematical approximation is valid, or due to the invalidity of the approximation, where the data fits well Eq. S2.

17.2. All unprocessed data – upper limit for the error in the scaling.

Above, we analyzed superconductivity in each of the materials individually, demonstrating mostly agreement with Eq. 1, while discussing briefly the superconducting characteristic of the specific films. As a part of this analysis, we sometimes had to neglect some of the films due to uncertainty in the values we presented in the above tables. Here we would like to present all the data, as is, without processing it (despite some cases of large errors in the data extraction process). One can see that the linearity of dT_c vs. R_s on a log-log scale (Fig. S17.2) is still convincing. Yet, at the bottom right side of the graph, some of the data sets curve down faster than a power law. A closer look at these materials reveals that this rapid decrease occurs mainly in Al, Bi and Pb films, all were grown by Goldman and co-authors [7,12,14], as well as some of the samples grown by Strongin *et al.* [6]. The immediate direct relation between these films is the fact that they all were grown on conducting substrates. Hence, this may have led to the fact that the superconductivity in

these films was affected by the proximity effect, so that Cooper pairs from the superconductor were freely hybridized with electrons from the conductive substrate.

Although Eq. 1 does seem to describe well also sets of films in which the proximity effect is the governing mechanism for the change in T_c , *e.g.*, in the case of the discussed Nb films [24], it may be that here, there are two dominant mechanisms that govern T_c . That is, for thicker films, the proximity effect may be negligible, and therefore only one mechanism dominates T_c , resulting in an agreement of the data with Eq. 1. On the other hand, for the thinner films, the proximity effect may become gradually more significant, competing with the mechanism that is dominant in the thicker films. Such dual dominancy of two competing mechanisms may lead to complex behavior that deviates from the conventional simple form. Indeed, Fig. S17.2 demonstrates that the linearity of the data for these films (on log-log axes) is valid for most of the scale, while dT_c decays faster than linear beginning from a certain thickness value, which is material dependent. This may suggest that an additional mechanism that changes T_c is introduced at the thinner films. In fact, the Goldman and co-authors indeed reported that for the thinnest films, they suspect that the Ge substrate upon which they grow their films [7,12,14] proximitizes the deposited superconducting films. They used this explanation to support their observation of finite T_c for films measured to be thinner than a single atomic unit cell.

Despite the current discussion, we cannot eliminate the other two potential explanations for the deviation of the thinner films from Eq. 1 in these sets of data: (a) there is a consistent measurement error (this explanation complies also with the observation of finite T_c for films thinner than the unit cell); and (b) Eq. 1 has an unknown limit and is not valid below a certain thickness (such limitation of Eq. 1 cannot explain the existence of superconductivity in films thinner than a single unit cell).

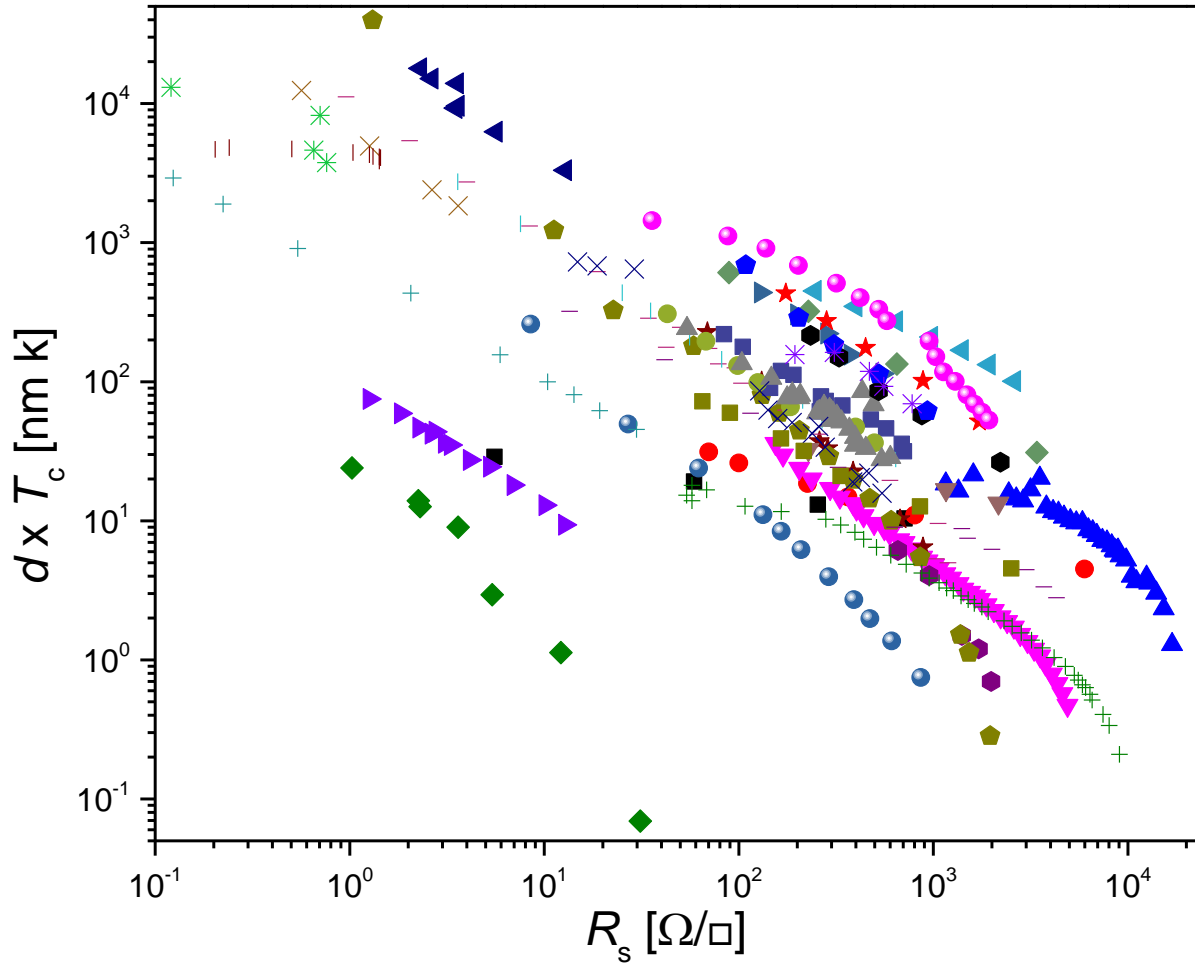


Fig. S17.2. dT_c vs. R_s for all unprocessed data presented and discussed in the paper. A collection of all the data presented and discussed above, regardless of the level of certainty in the values, and despite the potential sources of errors that are discussed in the introduction to the Supplemental Material. Yet, universality of Eq. 1 can be realized even here, in comparison, for example, to Fig. 5c-e. A concave down decrease of some of the data sets is likely to be due to measurement error and underestimation of the thickness values or the proximization with conducting substrate upon which the superconducting films was deposited. In this plot, we used the following symbols: ■ Al from Cohen and Abeles [5]; ● Al from in Strongin *et al.* [6]; ▲ Al from Haviland, Liu and Goldman [12]; ▼ Bi [12]; ◆ CoSi₂ [13]; ◀ MgB₂ [15]; ▶ Mo [16]; ◆

α MoGe by Yazdani and Kapitulnik [21]; \star α MoGe from Graybeal and co-authors [18–20]; \blacklozenge α MoGe from Graybeal and Beasley [40]; $+$ Nb [24]; \times α Nb₃Ge [25]; \ast Nb₃Sn [26]; $-$ NbN from Wang and co-authors [27,29]; $|$ NbN from Miki, Wang and co-authors [28]; \blacksquare NbN by Semenov *et al.* [30]; \bullet NbN by Kang *et al.* [31]; \blacktriangledown NbN by Belacour *et al.* [32]; \blacktriangle our NbN films; \blacklozenge , \blacktriangleleft , \blacktriangleright , \blacklozenge , \star , \blacklozenge and \bullet are Pb films by Strongin *et al.* that correspond to triangles facing down, triangles facing up, circles with an ‘x’, large circles, small circles, empty circles and empty triangles facing up in [6]; $+$ Pb by Haviland, Liu and Goldman [12]; \times α ReW [34]; \ast Sn [6]; $-$ disordered TiN by Klapwijk and co-authors [37,38], $|$ V₃Si [26], and \blacksquare are disordered TiN by Baturina and co-authors [37].

References

- [1] D. I. version 1.6, [Http://datathief.org](http://datathief.org) B. Tummens, (2006).
- [2] C. Strunk, C. Sürgers, U. Paschen, and H. Löhneysen, *Phys. Rev. B* **49**, 4053 (1994).
- [3] W. Siemons, M. Steiner, G. Koster, D. Blank, M. Beasley, and A. Kapitulnik, *Phys. Rev. B* **77**, 174506 (2008).
- [4] B. Matthias, T. Geballe, and V. Compton, *Rev. Mod. Phys.* **35**, 1 (1963).
- [5] R. Cohen and B. Abeles, *Phys. Rev.* **109**, 444 (1968).
- [6] M. Strongin, R. Thompson, O. Kammerer, and J. Crow, *Phys. Rev. B* **1**, 1078 (1970).
- [7] Y. Liu, D. B. Haviland, B. Nease, and A. M. Goldman, *Phys. Rev. B* **47**, 5931 (1993).
- [8] I. L. Landau, D. L. Shapovalov, and I. A. Parshin, *JETP Lett.* **53**, 263 (1991).
- [9] R. P. Silverman, *Phys. Rev. B* **16**, 2066 (1977).
- [10] R. P. Silverman, *Phys. Rev. B* **19**, 233 (1979).
- [11] D. G. Naugle, R. E. Glover III, and W. Moorman, *Physica* **32**, 250 (1971).
- [12] D. B. Haviland, Y. Liu, and A. M. Goldman, *Phys. Rev. Lett.* **62**, 2180 (1989).

- [13] P. A. Badoz, A. Briggs, E. Rosencher, F. A. D'Avitaya, and C. D'Anterrosches, *Appl. Phys. Lett.* **51**, 169 (1987).
- [14] H. M. Jaeger, D. B. Haviland, B. G. Orr, and A. M. Goldman, *Phys. Rev. B* **40**, 182 (1989).
- [15] a. V. Pogrebnyakov, J. M. Redwing, J. E. Jones, X. X. Xi, S. Y. Xu, Q. Li, V. Vaithyanathan, and D. G. Schlom, *Appl. Phys. Lett.* **82**, 4319 (2003).
- [16] L. Fàbrega, a Camón, I. Fernández-Martínez, J. Sesé, M. Parra-Borderías, O. Gil, R. González-Arrabal, J. L. Costa-Krämer, and F. Briones, *Supercond. Sci. Technol.* **24**, 075014 (2011).
- [17] J. M. Graybeal and M. R. Beasley, *Phys. Rev. B* **29**, 4167 (1984).
- [18] H. Tashiro, J. Graybeal, D. Tanner, E. Nicol, J. Carbotte, and G. Carr, *Phys. Rev. B* **78**, 014509 (2008).
- [19] S. Turneaure, T. Lemberger, and J. Graybeal, *Phys. Rev. B* **63**, 174505 (2001).
- [20] S. Turneaure, T. Lemberger, and J. Graybeal, *Phys. Rev. B* **64**, 179901 (2001).
- [21] A. Yazdani and A. Kapitulnik, *Phys. Rev. Lett.* **74**, 3037 (2000).
- [22] A. M. Finkel'stein, *Phys. B Condens. Matter* **197**, 636 (1994).
- [23] J. M. Graybeal, *Phys. B+C* **135**, 113 (1985).
- [24] A. Gubin, K. Il'in, S. Vitusevich, M. Siegel, and N. Klein, *Phys. Rev. B* **72**, 064503 (2005).
- [25] H. Kes and C. C. Tsuei, *Phys. Rev. B* **28**, 5126 (1983).
- [26] T. Orlando, E. McNiff, S. Foner, and M. Beasley, *Phys. Rev. B* **19**, 4545 (1979).
- [27] Z. Wang, A. Kawakami, Y. Uzawa, and B. Komiyama, *J. Appl. Phys.* **79**, 7837 (1996).
- [28] S. Miki, Y. Uzawa, A. Kawakami, and Z. Wang, *Electron. Commun. Japan (Part II Electronincs)* **85**, 77 (2002).
- [29] S. Ezaki, K. Makise, B. Shinozaki, T. Odo, T. Asano, H. Terai, T. Yamashita, S. Miki, and Z. Wang, *J. Phys. Condens. Matter* **24**, 475702 (2012).
- [30] a. Semenov, B. Günther, U. Böttger, H.-W. Hübers, H. Bartolf, a. Engel, a. Schilling, K. Ilin, M. Siegel, R. Schneider, D. Gerthsen, and N. Gippius, *Phys. Rev. B* **80**, 054510 (2009).

- [31] L. Kang, B. B. Jin, X. Y. Liu, X. Q. Jia, J. Chen, Z. M. Ji, W. W. Xu, P. H. Wu, S. B. Mi, a. Pimenov, Y. J. Wu, and B. G. Wang, *J. Appl. Phys.* **109**, 033908 (2011).
- [32] C. Delacour, L. Ortega, M. Faucher, T. Crozes, T. Fournier, B. Pannetier, and V. Bouchiat, *Phys. Rev. B* **83**, 144504 (2011).
- [33] B. H. Müller, T. Schmidt, and M. Henzler, *Surf. Sci.* **376**, 123 (1997).
- [34] H. Raffy, R. Laibowitz, P. Chaudhari, and S. Maekawa, *Phys. Rev. B* **28**, 6607 (1983).
- [35] S. Maekawa and H. Fukuyama, *J. Phys. Soc. Japan* **51**, 1380 (1982).
- [36] V. M. Vinokur, T. I. Baturina, M. V. Fistul, A. Y. Mironov, M. R. Baklanov, and C. Strunk, *Nature* **452**, 613 (2008).
- [37] E. F. C. Driessen, P. C. J. J. Coumou, R. R. Tromp, P. J. de Visser, and T. M. Klapwijk, *Phys. Rev. Lett.* **109**, 107003 (2012).
- [38] P. C. J. J. Coumou, E. F. C. Driessen, J. Bueno, C. Chapelier, and T. M. Klapwijk, *Phys. Rev. B* **88**, 180505(R) (2013).
- [39] T. I. Baturina and S. V. Postolova, in *Int. Work. Strongly Disord. Supercond. Supercond. Insul. Transit.* (2104), Villard de Lans, France.
- [40] J. M. Graybeal, *Phys. B+C* **135**, 113 (1985).